Experimental Neurology 279 (2016) 243–260

Contents lists available at ScienceDirect

Experimental Neurology

journal homepage: www.elsevier.com/locate/yexnr

Research Paper

The multiple sclerosis drug fingolimod (FTY720) stimulates neuronal gene expression, axonal growth and regeneration

Sofia Anastasiadou, Bernd Knöll *

Institute of Physiological Chemistry, Ulm University, Albert-Einstein-Allee 11, 89081 Ulm, Germany

ARTICLE INFO

Article history:
Received 16 November 2015
Received in revised form 3 March 2016
Accepted 11 March 2016
Available online 12 March 2016

Keywords:
Fingolimod
FTY720
Multiple sclerosis
IEG
c-Fos
SRF
Sphingosine
Neurite growth
Growth cone
Axon regeneration
Neurodegeneration

ABSTRACT

Fingolimod (FTY720) is a new generation oral treatment for multiple sclerosis (MS). So far, FTY720 was mainly considered to target trafficking of immune cells but not brain cells such as neurons. Herein, we analyzed FTY720's potential to directly alter neuronal function. In CNS neurons, we identified a FTY720 governed gene expression response. FTY720 upregulated immediate early genes (IEGs) encoding for neuronal activity associated transcription factors such as *c-Fos*, *FosB*, *Egr1* and *Egr2* and induced actin cytoskeleton associated genes (actin isoforms, tropomyosin, calponin). Stimulation of primary neurons with FTY720 enhanced neurite growth and altered growth cone morphology. In accordance, FTY720 enhanced axon regeneration in mice upon facial nerve axotomy. We identified components of a FTY720 engaged signaling cascade including S1P receptors, G12/13 G-proteins, RhoA-GTPases and the transcription factors SRF/MRTF.

In summary, we uncovered a broader cellular and therapeutic operation mode of FTY720, suggesting beneficial FTY720 effects also on CNS neurons during MS therapy and for treatment of other neurodegenerative diseases requiring neuroprotective and neurorestorative processes.

1. Introduction

Fingolimod (FTY720) is a novel drug for patients with relapsing remitting MS (Brinkmann et al., 2010; Pelletier and Hafler, 2012; Sanford, 2014). Mechanistically, FTY720 exerts its beneficial function through preventing CNS entry of auto-immune lymphocytes (Brinkmann et al., 2010; Brunkhorst et al., 2014; Chun and Hartung, 2010). FTY720 as well as its analog sphingosine are phosphorylated *in vivo* by sphingosine kinases (SphK) to produce the biologically active molecules, sphingosine-1-phosphate (S1P) or FTY720-phosphate (FTY720-P). Similar to S1P, active FTY720 engages several G protein coupled S1P receptors. Besides its peripheral immune modulatory functions, FTY720 was attributed beneficial effects directly on the CNS (Ingwersen et al., 2012). FTY720 has a neuroprotective impact in various murine disease models (Brunkhorst et al., 2014) including neuroinflammation associated with axonal injury (Lee et al., 2009), ischemia (Hasegawa et al., 2010; Wei et al., 2011), prion (Moon et al., 2013) or β-amyloid toxicity (Takasugi et al., 2013), exitotoxicity (Deogracias et al., 2012; Di Menna et al., 2013) and Rett syndrome (Deogracias et al., 2012). In the latter two reports, brain derived neurotrophic factor (BDNF) was identified as mediator of FTY720 activity (Deogracias et al., 2012; Di Menna et al., 2013). FTY720 modulates de- and/or remyelination in MS mouse models, although the exact cellular target (*e.g.* neurons or glia) of FTY720 action is difficult to decipher (Blanc et al., 2014; Choi et al., 2011; Kim et al., 2011; Papadopoulos et al., 2010). Recent data suggest an axonoprotective FTY720 function (Slowik et al., 2014). Nevertheless, data of FTY720 action on neurons are sparse and the impact of FTY720 on neurons is just at the beginning of being analyzed in depth. Spiegel and colleagues recently reported that FTY720 inhibits specific histone deacetylases (HDACs) in neurons (Hait et al., 2014). Such epigenetic alterations suggest that FTY720 mediates distinct neuronal gene expression programs, potentially involving the gene regulator CREB (Deogracias et al., 2012). However, detailed molecular and cellular insights on FTY720's mechanism of modulating such neuronal functions are currently not available. In astrocytes (Cui et al., 2014; Osinde et al., 2007) or Schwann cells (Heinen et al., 2015), FTY720 was reported to modulate specific gene expression programs.

In this study we report that FTY720 elicits a neuronal gene expression response, resulting in induction of neuronal activity connected genes including the immediate early genes (IEG) *c-Fos*, *FosB*, *Bdnf*, *Egr1* and *Egr2*. In addition, FTY720 induced genes encoding for components of the actin cytoskeleton. In agreement, FTY720 modulated the morphology of actin-rich neuronal growth cones and stimulated neurite growth *in vitro* as well as axonal regeneration *in vivo*. FTY720's potential

* Corresponding author.
E-mail address: bernd.knoell@uni-ulm.de (B. Knöll).

http://dx.doi.org/10.1016/j.expneurol.2016.03.012

to modulate neuronal gene expression and morphology involved a S1P receptor-G12/13-RhoA dependent signaling cascade and the transcription factor serum response factor (SRF), a neuroprotective gene regulator. SRF is an established neuronal activity induced transcription factor conveying a neuronal IEG response (Knoll and Nordheim, 2009; Ramanan et al., 2005). For regulation of IEGs, MAP kinase signaling stimulates an SRF interaction with cofactors of the TCF family including Elk-1 (Knoll and Nordheim, 2009; Posern and Treisman, 2006). Besides IEGs, SRF is intimately connected with the regulation of cellular actin dynamics and, in turn, SRF activity is also adjusted by the cellular actin equilibrium and Rho-GTPases (Olson and Nordheim, 2010). Several SRF target genes encode for actin isoforms (*e.g. Acta*, *Actb*) and actin binding proteins (ABPs) such as tropomyosin and calponin. A further ABP regulated by SRF is the actin severing factor cofilin (Alberti et al., 2005; Beck et al., 2012), known to modulate neuronal actin dynamics (Flynn et al., 2012). Here, SRF teams up with a second class of cofactors, myocardin related transcription factors (MRTFs), whose activity is adjusted by Rho-GTPases and changes in the cellular G- to F-actin ratio (Olson and Nordheim, 2010). SRF-deficient neurons display altered actin dynamics and aberrant growth cone structures. In addition, SRF stimulates various aspects of neuronal cell motility including axon growth (Knoll and Nordheim, 2009; Olson and Nordheim, 2010) and PNS axon regeneration (Stern et al., 2013; Stern and Knoll, 2014). SRF deficiency also affects myelin de- and regeneration in mouse models of demyelination (Anastasiadou et al., 2015).

Herein we present a direct FTY720 impact on neurons, suggesting that FTY720 medication impinges on both immune cell as well as neuronal function. This finding is of potential interest not only for MS therapy but also for the therapy of other neurological diseases aiming at restoration of neuronal function.

2. Materials and methods

2.1. Neuronal cell culture

We used for all neuronal cell cultures C57BL/6 mice. Cerebellar cultures derived from postnatal day (P) four to five (P4–P5) mice were incubated in NMEM/B27 medium as described previously (Knoll et al., 2006). Adult DRG neurons were harvested from 6 to 8 week old mice and were cultured for 24 h with or without NGF (50 ng/ml; Peprotech) as indicated. For biochemical and qPCR analysis, cerebellar neurons (3×10^6) were cultured on poly-L-lysine (10 μg/ml; Sigma) and laminin (2 μg/ml; Gibco) coated 35 mm dishes. For immunocytochemisty, cerebellar (2.5×10^4) or DRG (5×10^3) neurons were plated on poly-L-lysine (100 μg/ml) and laminin (5 μg/ml) coated coverslips (13 mm).

For qPCR experiments, cerebellar neurons were treated with 2 μM FTY720 (Novartis, Switzerland; stock: 10 mM in DMSO) after 2 div (days *in vitro*) for 1, 8 or 24 h. BDNF (Peprotech) was applied to the culture medium of cerebellar neurons, grown for 2 div, at 10 ng/ml also for 1, 8 or 24 h. Diethyl fumarate (Sigma-Aldrich) was used at a final concentration of 10 μM. For neurite growth experiments (*e.g.* Fig. 3), neurons were grown in culture for a total duration of 24 h.

For Rho inhibition, we used the fusion toxin C2IN-C3lim at 300 ng/ml together with C2IIα at 600 ng/ml for 24 h (Barth et al., 1998). C2IN-C3lim/C2IIα was applied to cultures at 2 div. To ensure inhibition by C2IN-C3lim/C2IIα over the 24 h period, substances were added again into the medium 8 h after the first application. To deliver the Lsc-RGS (Moepps et al., 2008), MALΔNΔB1 (Miralles et al., 2003) or cofilin-GFP (Beck et al., 2012) expression vectors into neurons, we used nucleofection (Mirus) with 3 μg plasmid DNA for 4×10^6 cells. JTE-013 (Tocris), NIBR-0213 (Glixx Laboratories) and TY52156 (Tocris) were dissolved in DMSO and pre-incubated for 30 mins at 10 μM, 1 μM and 1 μM, respectively for gene expression studies. For neurite growth, inhibitors were applied for the entire duration of the experiment at 1 μM (JTE-013), 0.1 μM (NIBR-0213) and 0.1 μM (TY52156). S1P was dissolved in MeOH and applied at 1 μM. All inhibitors were added already 30 min before FTY720 or S1P administration to cultures.

For the downregulation of SRF and CREB *via* siRNA, we used the ON-TARGETplus SMARTpool siRNA (Dharmacon), L-050116-01 and L-040959-01, respectively. As control siRNA, we used the AllStars Neg. Control siRNA (Qiagen). All siRNAs were delivered into the neurons by nucleofection of 1 μM siRNA solution. Cells were kept 3 days in culture prior to stimulation with FTY720.

All antagonists and siRNAs are summarized in Table 1.

2.2. Facial nerve transection

Facial nerve transection was performed as described previously (Raivich et al., 2004; Stern et al., 2013). Adult C57BL/6 mice of either sex (approx. 12 weeks old) were anesthetized by inhalation of isoflurane, a skin incision was made behind the left ear, and the facial nerve was exposed. Afterwards, the nerve was transected with microscissors 2 mm posterior to the foramen stylomastoideum. The contralateral nerve was left intact and responses in this facial nucleus served as intra-animal control. Absence of eye-lid closure and whisker movement proved successful nerve transection. FTY720 (1 mg/kg body weight) or the same volume DMSO was i.p. injected every second day, starting one day after injury. Similar FTY720 concentrations were used by others (Choi et al., 2011; Hait et al., 2014; Kim et al., 2011). Regeneration of the facial nerve was quantified by retrograde axonal tracing with fluorogold (FG; Fluorochrome). For this, 4×1 μl of FG (4% in H_2O) was injected with a Hamilton syringe at multiple positions in each whisker pad 15 d after injury. After another 3 d, brains were dissected. FG-positive neurons of all sections of both facial nuclei per each animal were evaluated before immunohistological staining. Before and after facial nerve transection, animals were housed in groups in standard cages. Mice were maintained under specific pathogen-free conditions with free access to food and water in the animal facility (12-h light–dark cycle) of University of Ulm. All experiments were in accordance with institutional guidelines and German animal protection laws and were approved by the regional government authority (Number: 1232; Regierungspräsidium Tübingen, Germany).

2.3. Organotypic cerebellar cell culture

Cerebellar slices (350 μm) of P5 C57BL/6 wildtype mice were prepared with a tissue chopper (Bachhofer, Reutlingen, Germany). Subsequently, four slices were arranged on the membrane of a Millicell cell culture insert (PICMO3050; Millipore) placed in one well of a 6-well plate with 1 ml of NMEM/B27 medium. The next day, slices were stimulated by adding DMSO, FTY720 (2 μM) or BDNF (10 ng/ml) in the culture medium for 2 h, 8 h or 24 h as indicated in Fig. 2.

2.4. Immunocytochemisty

Cells were fixed for 15 min in 4% PFA/5% sucrose/PBS, permeabilized for 5 min in 0.1% Triton-X-100/PBS and blocked for 30 min in 2% BSA/PBS. The primary antibody against rabbit anti class III β-tubulin (1:1000; Covance; Cat. No. PRB-435P) was incubated overnight at 4 °C. The primary antibody was detected with a goat Alexa 488 conjugated secondary antibody (1:1500; Molecular Probes; Cat. No. A-11008). F-actin was stained with Texas Red-X Phalloidin (1:70; Molecular Probes) in the secondary antibody solution. Phalloidin labels F-actin in all cells, not only neurons, present in a culture and was used for quantification of the total number of neurons (βIII tubulin positive) in the cerebellar cultures (Supplementary Fig. 1).

2.5. Immunohistochemistry

Organotypic cultures were fixed with 4% paraformaldehyde (PFA) in PBS for 1 h at 4 °C, followed by preparation of 7 μm paraffin microtome

Table 1
Summary of reagents used.

Agent	Target	Supplier/company	Concentration	Application duration	Application time-point
C2IN-C3lim	RhoA-GTPases	Holger Barth Ulm University	300 ng/ml	1 div	After 2 div
Lsc-RGS	Gα12/13	Barbara Möpps Ulm University	Electroporation of 3 μg plasmid	2 div	Immediately when plating neurons
JTE-013	*S1PR2* receptor	Tocris Cat. No. 2392	10 μM (qPCR) 1 μM (neurite growth)	– 30 min (qPCR) – 1 div (neurite growth)	– 30 min before FTY stimulation (qPCR) – Immediately after plating (neurite growth)
NIBR-0213	*S1PR1* receptor	Glixx Laboratories Cat. No. GLXC-02221	1 μM (qPCR) 0.1 μM (neurite growth)	– 30 min (qPCR) – 1 div (neurite growth)	– 30 min before FTY stimulation (qPCR) – Immediately after plating (neurite growth)
TY52156	*S1PR3* receptor	Tocris Cat. No. 5328	1 μM (qPCR) 0.1 μM (neurite growth)	– 30 min (qPCR) – 1 div (neurite growth)	– 30 min before FTY stimulation (qPCR) – Immediately after plating (neurite growth)
siSrf	Mouse *Srf* mRNA	Dharmacon Cat. No. L-050116-01	Electroporation of 1 μM siRNA	3 div	– Immediately after plating
siCreb	Mouse *Creb* mRNA	Dharmacon Cat. No. L-040959-01	Electroporation of 1 μM siRNA	3 div	– Immediately after plating
Control siRNA	No mRNA target	Qiagen Cat. No. SI03650318	Electroporation of 1 μM siRNA	3 div	– Immediately after plating

slices. Immunohistochemistry was performed with the following primary antibodies: mouse anti-NeuN (1:500; Millipore; Cat. No. MAB377) and rabbit anti-*c-Fos* (1:10,000; Calbiochem; Cat. No. ABE457). Primary antibodies were detected with goat anti-mouse or rabbit Alexa 488 (Cat. No. A-11008 or A-11001) and Alexa 546 (Cat. No. A-11003 or A-11071) conjugated secondary antibodies (1:1500; all from Molecular Probes).

Brains were dissected in ice-cold PBS and fixed in 4% PFA for 3–4 days at 4 °C. Then, the tissue was dehydrated (2 × 70% EtOH, 2 × 90% EtOH, 2 × 100% EtOH, 3 × 100% Xylene, 3 × Paraffin; each 90 min), embedded in paraffin in plastic holders, followed by preparation of 5 μm paraffin microtome slices. After blocking with 2%BSA/PBS, sections were labeled with primary antibodies including anti-ATF3 (rabbit, 1:500; Santa Cruz Biotechnology; Cat. No. sc-188), anti-SMI-32 (mouse, 1:500; Millipore; Cat. No. NE1023), anti-FG (rabbit, 1:5000, Millipore; Cat. No AB153), anti-IBA1 (rabbit, 1:1000, Wako; Cat. No. 019-19741), anti-S100 (mouse, 1:1000; Abcam; Cat. No. Ab4066), anti-MBP (mouse, 1:2000; Covance; Cat. No. NE1018), anti-nestin (mouse, 1:1000; Chemicon; Cat. No. MAB353), anti-doublecortin (rabbit, 1:1000; Abcam; Cat. No Ab18723) and anti-GFAP (mouse, 1:1000; Santa Cruz; Cat. No. sc-33673). Detection of primary antibodies was performed using goat anti-mouse Biotin (1:500; Vector Laboratories; Cat. No. BA-9200) or Alexa Fluor (1:500; Invitrogen; see above) conjugated secondary antibodies and peroxidase-based detection systems using the ABC complex (Vector Laboratories) and DAB as substrate.

2.6. Biochemistry

Cells or brain slices were lysed in 100 mM Tris pH 7.8, 150 mM NaCl, 1 mM EDTA, 1% Triton-X-100, 1× protease inhibitors (Roche) and 1× PhosStop (Roche). Samples were resolved on 10% SDS-PAGE, followed by transfer on PVDF membranes (Amersham). After 1 h of blocking, first antibodies were applied overnight at 4 °C: rabbit anti-CREB (1:1000; Cell Signaling; Cat. No. 9197S), rabbit anti-P-CREB (1:1000; Cell Signaling; Cat. No. 9198S), rat anti-SRF (1:250; kindly provided by A. Nordheim, Tübingen University, Germany), mouse anti-GAPDH (1:60,000; Acris; Cat. No. OTI2D9), rabbit anti-c-Fos (1:1000; Santa Cruz; Cat. No. sc-52), rabbit anti-FosB (1:500; Santa Cruz; Cat. No: sc-48), rabbit anti-Egr1 (1:500; Santa Cruz; Cat. No. sc-110), rabbit anti-Cofilin (1:1000; Cell Signaling; Cat. No. 3312), rabbit anti-P-Cofilin (Serine 3; 1:1000; Cell Signaling; Cat. No. 3311) and rabbit anti-Egr2 (1:500; Covance; Cat. No. PRB-236P). Detection of first antibodies involved horseradish-peroxidase conjugated secondary antibodies (1:5000; Santa Cruz Biotechnology) and the ECL Western Blotting Substrate (Pierce). Membranes were exposed on X-ray films (Fujifilm) in a dark room and developed in an Agfa film processor (X-ray developer).

2.7. Quantitative real-time PCR (qPCR)

We isolated total RNA from P3-P5 postnatal cerebellar cell cultures grown for 2 div with the RNeasy kit (Qiagen). Reverse transcription was performed with 1 μg RNA using reverse transcriptase (Promega) and random hexamers. We performed qPCR on a Light Cycler 480II (Roche) with the Power PCR SYBR green PCR master mix (Takara). The LC480 II Software detects this threshold cycle value (Ct value) for each sample. The higher the Ct value, the lower the original cDNA amount for a certain gene in the sample. In order to neutralize potential variations in total mRNA amounts used for the cDNA synthesis, the Ct values of the house keeping gene *Gapdh* (glycerinaldehyd-3-phosphat- dehydrogenase) were used for normalization. The relative mRNA expression values of the control sample (DMSO treated) were set to 1.

Primer sequences:

Primer	Fwd primer sequence (5′ > 3′)	Rev primer sequence (5′ > 3′)
c-Fos	CCT GCC CCT TCT CAA CGA C	GCT CCA CGT TGC TGA TGC T
FosB	TAA TGT GCA GGA ACC GTC GG	TGC CTT TTC CTC TTC AAG CTG
Egr1	GCC GAG CGA ACA ACC CTA T	TCC ACC ATC GCC TTC TCA TT
Egr2	GTT GAC TGT CAC TCC AAG AAA TGG	AGC GCA GCC CTG TAG GC
Acta	CAG CAA ACA GGA ATA CGA CGA A	TGT GTG CTA GAG GCA GAG CAG
Tpm1a	CTG ATA AGA AGG CGG CGG	TCT TTT GCA GTG ACA CCA GCTC
Cnn	GAA GGT CAA TGA GTC AAC TCA GAA	CCA TAC TTG GTA ATG GCT TTG A
Tagln	GAT GTA GGC CGC CCA GAT C	ATC ACA CCA TTC TTC AGC CAC A
Bdnf	ACC ATA AGG ACG CGG ACT TG	GAG TAG AGG AGG CTC CAA AGG C
Ccl2	CCC AAT GAG TAG GCT GGA GA	TCT GGA CCC ATT CCT TCT TG
Ccl3	TGC CCT TGC TGT TCT TCT CT	GTG GAA TCT TCC GGC TGT AG
Ccl9	GGC ACA GCA AGG GCT TGA	GGA CAG GCA GCA ATC TGA AGA

2.8. Statistical analysis and quantification

The exact numbers (n) of independent cell cultures or animals are indicated in figure bars. For Fig. 1, the number of independent cell cultures analyzed for all panels is provided in Fig. 1F. In Fig. 2A–D, one culture was analyzed for each time-point. In Fig. 2E and F, organotypic

cultures derived from more than three animals were analyzed. In Fig. 3, the total number of growth cones, each marked by a circle, derived from three independent cultures is provided. For Figs. 4 and 6, seven animals were tested for each condition (control or FTY treated). In Fig. 5, the total number of neurons, each marked by a circle, derived from three independent cultures is provided. In Fig. 7, three to seven animals were tested for each condition as indicated in the bar graphs. For Fig. 8A, the number of independent cell cultures analyzed for all panels is provided in the bar graph. For Fig. 8B–J, the number of independent cell cultures analyzed for each panel is provided in Fig. 8B. In Fig. 8K, L, the total number of neurons, each marked by a circle, derived from three independent cultures is provided. For Fig. 9, the number of independent cell cultures analyzed for each panel is provided in Fig. 9A. In Fig. 10A, the number of independent cultures is presented in the bar graph. For Fig. 10B–J, the number of independent cell cultures analyzed for each panel is provided in Fig. 10B. For Fig. 10K–O, the total number of growth cones, each marked by a circle, derived from three independent cultures is provided.

For growth cone morphology (≥100 growth cones/condition) and quantification of neurite length, pictures were analyzed using Zeiss Axiovision software. Growth cone area was recognized by phalloidin staining labeling the growth cone F-actin content. Here, the area tool was used to mark the entire outline of each individual growth cone. In order to exclude false positive signals not derived from growth cones, a threshold was set to exclude objects < 5 μm^2 and >500 μm^2. The total pixel number/growth cone area calculated by the axiovision software was converted to μm^2. For filopodia number, the total number of filopodia of one growth cone was quantified. Only filopodia > 1 μm were counted. For neurite length, the maximal neurite length of an individual βIII tubulin neuron was manually traced with the measure curve spline tool of the Zeiss Axiovision software.

Statistical significance was calculated using Prism6 software with 2way ANOVA multiple comparison tests with *, **, *** indicating p ≤ 0.05, 0.01 and 0.001, respectively. All data show SD if not indicated otherwise.

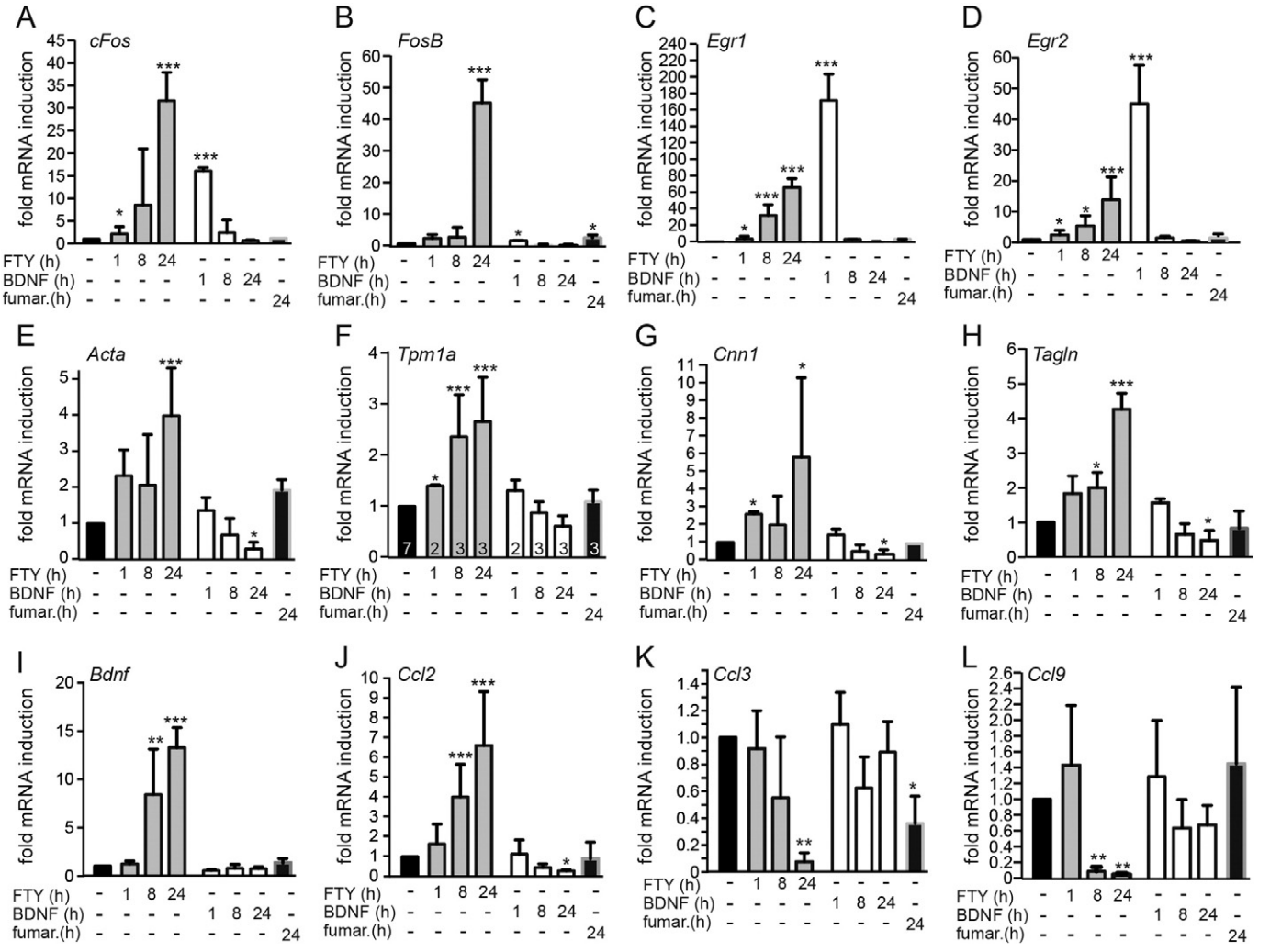

Fig. 1. FTY720 induces a neuronal gene expression response. Mouse cerebellar neurons were stimulated with the oral MS drugs FTY720 or diethyl fumarate ("fumar.") for time-points indicated. BDNF application was included as a positive control for IEG induction. Subsequently, qPCR was performed to quantify mRNA abundance of several immediate early genes (*c-Fos*, *FosB*, *Egr1*, *Egr2*, *Bdnf*), genes encoding components of the actin cytoskeleton (*Acta*, *Tpm1a*, *Cnn1* and *Tagln*) and CCL chemokines (*Ccl2*, *Ccl3*, *Ccl9*). Control values (DMSO control, first black bar) were set to 1 and fold induction is depicted. (A–D) FTY720 upregulated mRNA levels of all four IEGs tested. Overall, longer FTY720 application periods were more effective in IEG induction. BDNF application achieved IEG induction already at 1 h. Diethyl fumarate failed to modulate IEG levels. (E–H) All four actin associated genes were upregulated by FTY720. In contrast, BDNF reduced mRNA abundance of *Acta* (E), *Tpm1a* (F), *Cnn* (G) and *Tagln* (H). Fumarate had no obvious impact on actin cytoskeletal gene expression. (I) *Bdnf* mRNA abundance was elevated by FTY720, but not BDNF or fumarate administration. (J–L) The CCL chemokine family member *Ccl2* (J) was upregulated, whereas *Ccl3* (K) and *Ccl9* (L) were downregulated by FTY720. Numbers in bars in (F) indicate the number of independent cell cultures analyzed for each gene depicted in (A–L). Data are expressed as mean ± SD. Statistical significance was calculated in relation to the non-stimulated sample (first black bar in each panel).

3. Results

3.1. FTY720 induces a neuronal gene expression response

In order to analyze FTY720's potential to elicit a neuronal gene response, we used P3–P5 primary mouse cerebellar neurons (Fig. 1). These cultures consist of more than 90% (90.5 ± 1.5%; N = 3) of βIII tubulin positive neurons thereby reflecting almost exclusively neuronal responses (Supplementary Fig. 1). Cultures were treated with FTY720 for 1, 8 or 24 h. We used FTY720 in its unphosphorylated form at 2 μM, a concentration similarly used by other reports (Hait et al., 2014; Jackson et al., 2011; Takasugi et al., 2013). After cellular uptake, FTY720 is phosphorylated by SphK2 to P-FTY720 in many cell types, including neurons (Hait et al., 2014). We found robust *Sphk2* mRNA expression also in cerebellar neurons. *Sphk2* mRNA levels were not affected by FTY720 application (data not shown). In addition to FTY720, diethyl fumarate was employed, a further oral MS drug (Fox et al., 2014). We also included BDNF administration, known to elicit neuronal gene expression (Meier et al., 2011). After three days *in vitro* (div), cDNA prepared from cell cultures was subjected to qPCR allowing for quantitation of mRNA abundance of several immediate early genes (*c-Fos*, *FosB*, *Egr1*, *Egr2*, *Bdnf*). In order to analyze FTY720 induced modulation of actin-based neuronal motility, we examined mRNA abundance of genes encoding components of the actin cytoskeleton such as the actin isoform *Acta* (actin alpha 1, skeletal muscle). In addition, we analyzed ABPs of the calponin family, *Cnn1* (calponin1) and *Tagln* (transgelin), established regulators of actin-myosin interaction and tropomyosin (*Tpm1a*), an ABP enhancing actin polymerization and stabilizing actin filaments. Finally, we investigated whether FTY720 stimulates neuronal CCL chemokine abundance (*Ccl2*, *Ccl3*, *Ccl9*), established mediators of a brain resident immune response (Bose and Cho, 2013).

We observed that FTY720 administration resulted in a strong IEG response of *c-Fos* (Fig. 1A), *FosB* (Fig. 1B), *Egr1* (Fig. 1C) and *Egr2* (Fig. 1D) with maximal mRNA induction peaking 8 h–24 h after application. FTY720 application exceeded the well-known IEG inducer BDNF in *c-Fos* and *FosB* upregulation (Fig. 1A, B). Besides these four IEGs (Fig. 1A–D), FTY720 induced further IEGs including *Cyr61*, *Egr3*, *Npas4* and *Nr4a1* (Supplementary Fig. 2). In contrast, FTY720 did not alter *Srf* mRNA, SRF protein level or SRF phosphorylation (data not shown). In addition, we observed that FTY720 – but not BDNF – induced all actin cytoskeleton associated genes in a time dependent manner (Fig. 1E–H). FTY720 also upregulated *Bdnf* mRNA abundance (Fig. 1I) as reported before (Deogracias et al., 2012; Hait et al., 2014). Finally, we observed that FTY720 modulated neuronal mRNA abundance of CCL chemokines (Fig. 1J–L). FTY720 induced *Ccl2* mRNA levels (Fig. 1J), whereas other family members, *i.e. Ccl3* (Fig. 1K) and *Ccl9* (Fig. 1L) were downregulated. In contrast to FTY720, diethyl fumarate (fumar.) did not modulate mRNA abundance (Fig. 1A–L). This finding underscores the specificity of the FTY720 dependent gene expression response.

In order to corroborate findings on mRNA level (Fig. 1) we analyzed FTY720 mediated activity on neurons on protein level (Fig. 2). Here, we employed primary cerebellar cultures (Fig. 2A, B) as well as organotypic cerebellar brain slices of P5 mice reflecting more closely *in vivo* conditions (Fig. 2C-F). Samples were incubated with DMSO (as control), FTY720 or BDNF as positive control (Fig. 2). Subsequently, cell lysates were prepared and immunoblotting experiments with antibodies directed against c-Fos, FosB, Egr1 and Egr2 were performed (Fig. 2A–D). In agreement with the results obtained on mRNA level (Fig. 1), we noted upregulation of c-Fos, FosB, Egr1 and Egr2 protein levels after FTY720 application in both primary cerebellar neurons (Fig. 2A and B) and cerebellar organotypic slices (Fig. 2C and D).

In cerebellar neurons, FTY720 upregulated c-Fos and Egr1 similarly to effects observed for BDNF (Fig. 2A and B). FTY720 also upregulated FosB and Egr2, a finding not observed for BDNF stimulation in cerebellar neurons (Fig. 2A and B). In cerebellar slices, FTY720's potential to induce protein abundance of these IEGs was comparable to (c-Fos, FosB, Egr1) or exceeded (Egr2) *BDNF*'s impact on protein expression of these genes (Fig. 2C, D).

In addition, to immunoblotting (Fig. 2A–D), we performed immunohistochemical inspection of paraffin sections derived from these organotypic cerebellar brain slices (Fig. 2E and F). Upon treatment with DMSO (control; Fig. 2E) or FTY720 for 8 h (Fig. 2F), sections were labeled for c-Fos expression along with NeuN to identify neurons. In control treated cerebellar slices, no c-Fos expression was detectable (Fig. 2E). In contrast, FTY720 administration resulted in c-Fos upregulation in NeuN positive neurons (yellow neurons labeled with arrows in Fig. 2F).

In summary, we describe a several gene classes encompassing neuronal gene expression response elicited by FTY720.

3.2. FTY720 modulates neurite growth and growth cone morphology

Signaling by S1P, but so far not FTY720, was reported to modulate axon growth and morphology of growth cones consisting of F-actin rich finger-like filopodia (Fincher et al., 2014; Strochlic et al., 2008). FTY720 induced genes encoding for components of the actin cytoskeleton (Fig. 1). This tempted us to analyze whether FTY720 modulates neurite growth and growth cone morphology (Fig. 3). Neurons were identified by neuron-specific βIII tubulin expression and F-actin in growth cones was visualized with phalloidin.

First of all, we determined the impact of FTY720 application on cerebellar neurite growth (Fig. 3A–E). Notably, compared to control cultures treated with DMSO (Fig. 3A), FTY720 administration for 24 h (Fig. 3B) resulted in increased neurite growth. In a concentration range between 10 and 50 nM FTY720 stimulated neurite growth in a concentration-dependent manner, whereas higher concentrations (100 nM) reduced neurite length (Fig. 3E). Of note, BDNF application for 24 h also increased neurite growth (Fig. 3C and E), whereas co-application of FTY720 with BDNF decreased neurite length (Fig. 3D and E).

Similar to neurite growth, we observed that FTY720 administration (Fig. 3B') resulted in a concentration- and time-dependent increase of growth cone area (Fig. 3F) and filopodia number (Fig. 3G) compared to DMSO (Fig. 3A'). In fact, FTY720's activity on growth cones was comparable to BDNF (Meier et al., 2011). As seen for neurite growth, FTY720 and BDNF co-administration resulted in decreased growth cone area and filopodia number (Fig. 3D′, F and G).

Taken together, FTY720 can increase neurite growth, growth cone area and filopodia number in primary neurons.

3.3. FTY720 stimulates axon regeneration upon facial nerve injury

Upon nerve injury, the extent of axonal regeneration depends on the potential of axotomized neurons to re-initiate axon growth and convert growth-inert retraction bulbs into dynamic growth cones (Bradke et al., 2012). Given FTY720's potential to stimulate neurite growth and growth cone filopodia extension in primary neurons (Fig. 3), we examined whether FTY720 might likewise stimulate axon regeneration *in vivo* (Fig. 4). For this, we employed the facial nerve lesion model in mice (Moran and Graeber, 2004). The facial nerve connects motoneurons residing in facial nuclei of the brainstem with facial muscles controlling *e.g.* whisker and eyelid movements (see Fig. 4A). Axonal regeneration was quantified by fluorogold (FG) tracer injection into both whisker pads 15 days after unilateral nerve transection. After three days of retrograde tracer transport, facial motoneurons (encircled in black in Fig. 4A) incorporate the tracer, provided that nerve fibers were re-connected (red in Fig. 4A). For quantification, the percentage of regenerated motoneurons was determined by calculating the ratio between FG numbers on the lesioned and the unlesioned side. FTY720, or as control DMSO, was administered by intraperitoneal injection every second day along the entire experiment (n = 7 mice each group; see time-line in Fig. 4A).

Administration of FTY720 to mice was reported before to result in FTY720 brain accumulation (Hait et al., 2014).

In control DMSO injected mice (Fig. 4D), approximately 30% of neurons (quantified in Fig. 4V) regenerated after a total of 18 days. In contrast, in FTY720 injected mice, the number of FG positive motoneurons (arrows in Fig. 4E), indicative of successful axon regeneration, was almost doubled (Fig. 4V). This was corroborated by more ATF3 positive motoneurons present upon FTY720 treatment on the lesioned side (Supplementary

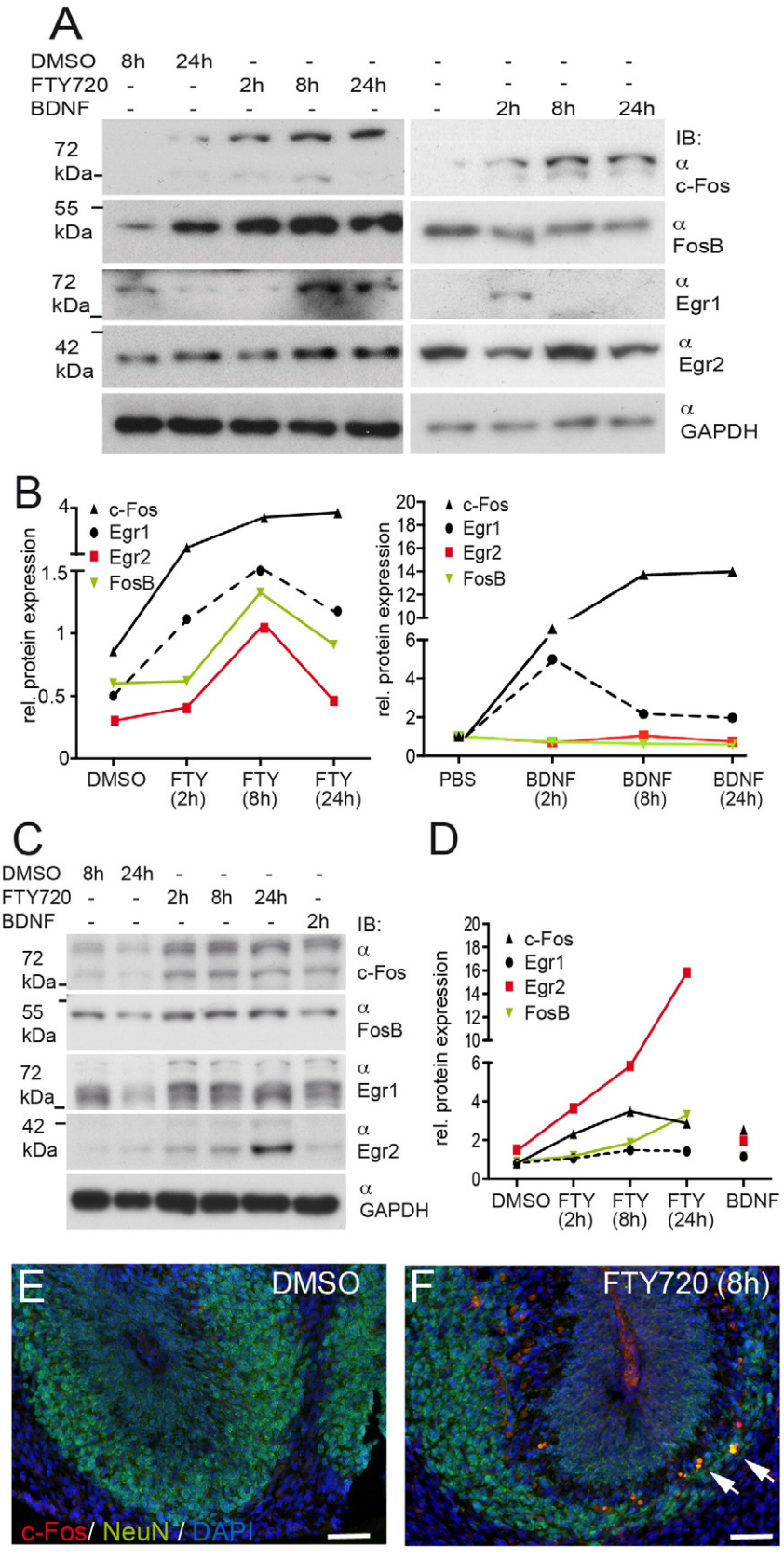

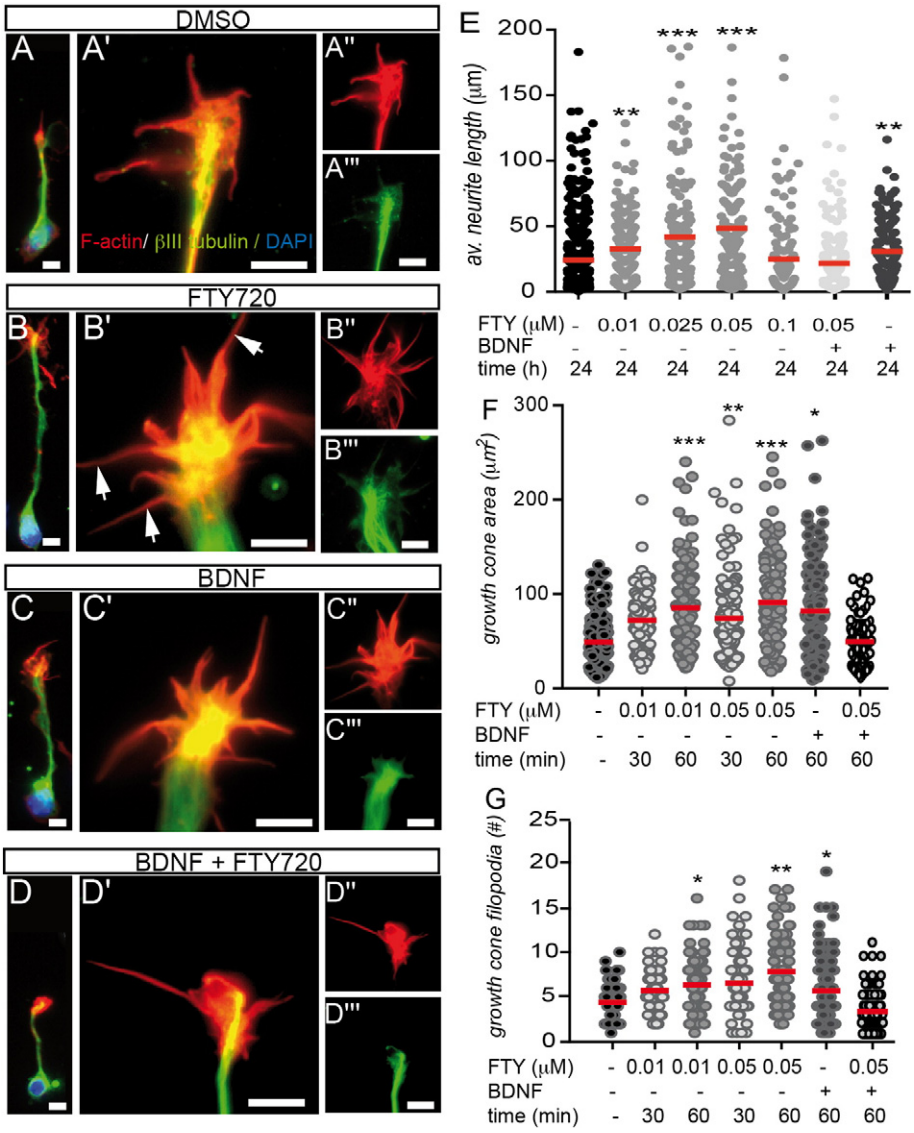

Fig. 3. FTY720 stimulates neurite growth and modifies neuronal growth cone morphology. Cerebellar neurons were treated with indicated concentrations and times of FTY720 or BDNF. Subsequently, neurons were labeled for F-actin (red) and βIII tubulin (green). (A) Entire neuron (A) and growth cone (A′) of control neuron treated with DMSO only. (A″ and A‴) represent individual channels of F-actin (A″) and βIII tubulin (A‴) also shown in the merged picture in (A′). (B) FTY720 treatment increased the neurite length (B) and overall growth cone area and number of F-actin positive filopodia (B′–B″). Individual filopodia are marked by arrows in B′. (C) Similar to FTY720 (B), application of BDNF enhanced neurite growth (C) and growth cone area as well as filopodia number (C′–C‴). (D) Co-administration of *BDNF* and FTY720 resulted in decreased neurite growth (D) and growth cone area and filopodia number (D′-D‴) compared to individual treatment (B and C). (E) Quantification of average neurite length after 24 h incubation with agents. (F and G) Quantification of growth cone area (F) or number of filopodia/growth cone (G) for the different conditions. In (E–G) represents every individual circle a single neuron (E) or growth cone (F and G) derived from one of at least three independent experiments. Statistical significance was calculated in relation to the DMSO treated control cultures. In conditions labeled with FTY in (E–G), "-"signifies DMSO treatment. The red lines indicate the mean values. Scale-bar (A–D; A′–D′) = 10 μm; (A″–D″; A‴–D‴) = 5 μm.

Fig. 3). ATF3 is a regeneration associated gene (RAG) encoding for a neuroprotective transcription factor (Hunt et al., 2012; Seijffers et al., 2007). FTY720 also induced *Atf3* mRNA abundance in primary neurons (Supplementary Fig. 3).

To monitor a potential neurodegenerative response, we quantified numbers of motoneurons positive for SMI-32, a marker associated with neurodegeneration (Laskawi and Wolff, 1996). On the unlesioned side, the number of SMI-32 positive neurons was expectedly low (Fig. 4F and G). In opposite to this, on the lesioned side, we noted more SMI-32 positive neurons (Fig. 4H and I). We also observed a consistent but statistically not significant SMI-32 reduction in the FTY720 treated animal group (Fig. 4I), compared to the DMSO group (Fig. 4H; quantified in Fig. 4W). This indicates reduced motoneuron degeneration upon injury by FTY720.

Fig. 2. FTY720 upregulates IEG protein levels in cerebellar brain slices and primary cerebellar cultures. (A) Cerebellar cultures were stimulated with FTY720 or BDNF for time-points indicated. FTY720 treatment upregulated protein abundance of c-Fos and Egr1 similar to BDNF, whereas FTY720, but not BDNF, resulted in enhanced FosB and Egr2 protein levels. (B) Quantification of protein levels in relation to GAPDH. (C) P5 organotypic cerebellar brain cultures were stimulated with FTY720, DMSO (control) or BDNF for time-points indicated. Subsequently, protein lysates were subjected to immunoblotting experiments using antibodies indicated. Stimulation with FTY720 resulted in elevated protein levels of all four IEGs, c-Fos, FosB, Egr1 and Egr2 at all time-points investigated. BDNF application also resulted in an increase of IEG protein abundance. (D) Quantification of protein levels normalized to GAPDH relative to DMSO control set to 1. (E and F) Paraffin sections of organotypic cerebellar brain slices, incubated with DMSO (E) or FTY720 (F) were labeled with anti-c-Fos (red) and anti-NeuN (green) directed antibodies along with DAPI (blue) to stain cell nuclei. After 8 h of FTY720 treatment (F), individual c-Fos positive neurons (yellow, see arrows in F) were detectable in comparison to control DMSO treated slices (E). Scale-bar (E, F) = 100 μm.

As FTY720 is a well-known modulator of immune cell responses, we analyzed whether FTY720 altered microglia (Fig. 4J–M) and astrocyte (Fig. 4N–Q) activation in the deafferented facial nuclei (quantified in Fig. 4X and Y). We noted a strong increase in the number of IBA-positive microglia (Fig. 4L and M) and GFAP-positive astrocytes (Fig. 4P and Q) on the injured side compared to unlesioned facial nuclei (Fig. 4J, K, N and O). However, this immune cell activation was comparable in DMSO and FTY720 treated animals (compare Fig. 4L and M and Fig. 4P

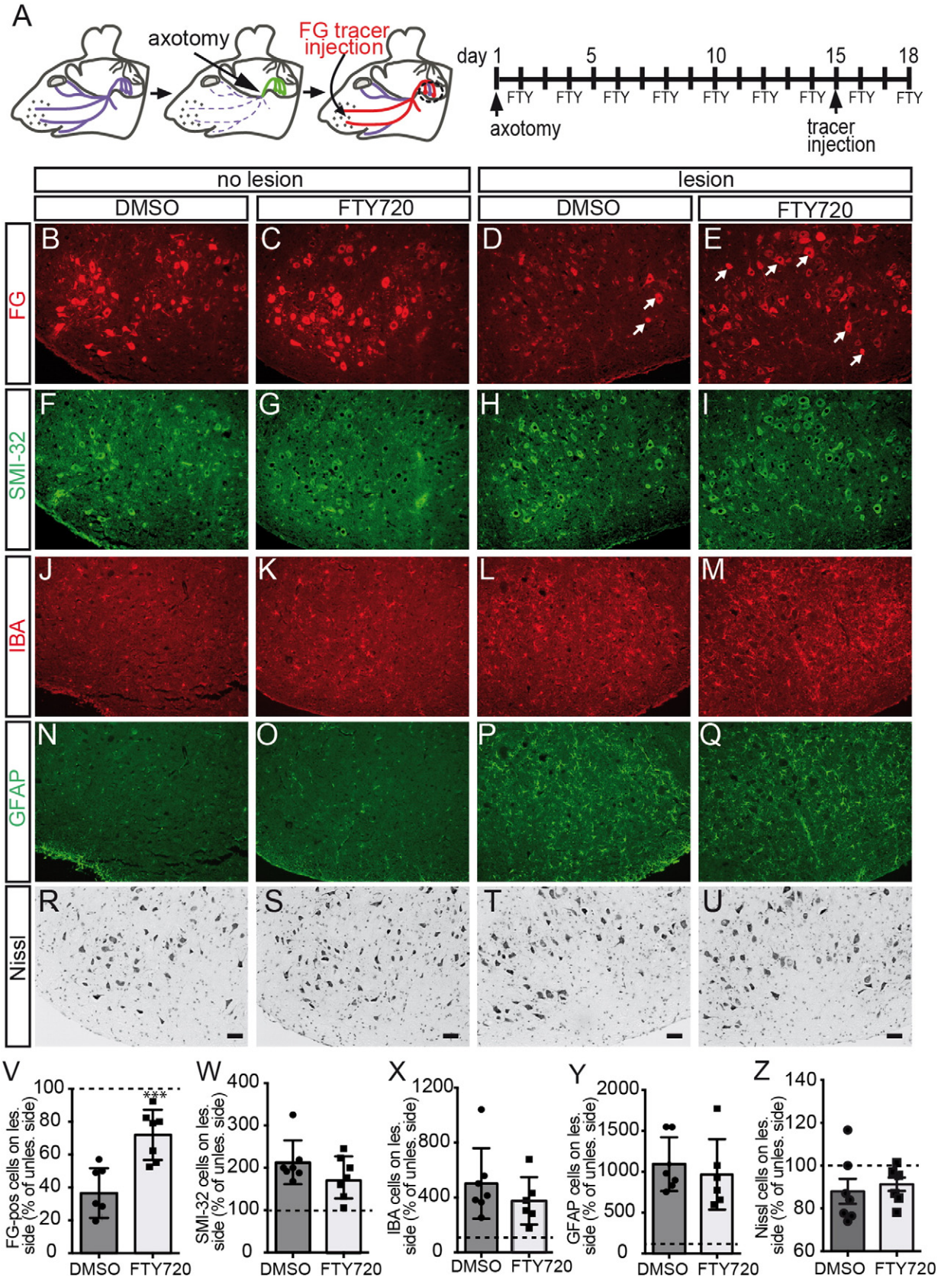

and Q), suggesting that FTY720 does not obviously impinge on axonal regeneration through modulation of brain resident immune response.

An obvious cause affecting axonal regeneration would be differential motoneuron loss between experimental groups upon injury. For this, we determined the number of Nissl positive motoneurons on the lesioned side in relation to the unlesioned side (set to 100%). This quantification revealed a motoneuron loss of approximately 10% on the lesioned compared to the intact facial nucleus in both DMSO and FTY720 treated animals (Fig. 4R–U and Z).

FTY720 might enhance axonal regeneration through direct stimulation of neurite growth, as demonstrated for primary cerebellar neurons before (Fig. 3). As facial nerve lesion is a model system of PNS injury, we analyzed whether FTY720 might also enhance neurite growth of PNS neurons (Fig. 5). For this, we cultured adult mouse DRG neurons in the presence of FTY720. As a positive control, we applied nerve growth factor (NGF), an established stimulator of DRG neurite growth (Fig. 5B).

Similar to CNS neurons (Fig. 3), FTY720 administration resulted in increased DRG neurite growth (Fig. 5C; quantified in E–G). Interestingly, co-application of NGF and FTY720 further enhanced neurite growth compared to individual application (Fig. 5D).

In summary, individual FTY720 incubation or a combined treatment of DRG neurons with NGF and FTY720 stimulated PNS neuron growth.

FTY720 modulates the extent of myelination in rodent MS models (Blanc et al., 2014; Choi et al., 2011; Kim et al., 2011; Papadopoulos et al., 2010). In order to analyze whether FTY720 modulates myelination processes after PNS nerve injury, we inspected the facial nerve for Schwann cells and myelin content (Fig. 6).

At 18 days post injury, signals of S100β positive Schwann cells were comparable between intact and injured nerve of control treated animals (Fig. 6A and C). In contrast, we observed an increased number of Schwann cell signals upon FTY720 treatment in the intact nerve (Fig. 6B) and even more Schwann cells in the lesioned nerve (Fig. 6D; quantified in Fig. 6I). Inspection of myelin levels with anti-MBP (myelin basic protein) directed antibodies revealed comparable myelin content in unlesioned nerves of control and FTY720 treated mice (Fig. 6E and F). Upon nerve injury, MBP signals were reduced in lesioned nerves of control treated animals (Fig. 6G). In contrast, in injured facial nerves of FTY720 treated animals, MBP levels were increased compared to control animals (Fig. 6H; quantified in J).

In summary, we here describe a first stimulatory FTY720 function in peripheral axon regeneration.

3.4. FTY720's impact on neurogenesis in the hippocampus and subventricular zone (SVZ)

Sphingosine signaling was previously connected to neurogenesis (McGiffert et al., 2002; Mizugishi et al., 2005). Thus, we were interested to analyze whether FTY720 administration over more than 2 weeks (see Fig. 4A) might affect adult neurogenesis. For this, we performed immunehistological staining (Fig. 7) with the type 1 stem cell marker nestin and doublecortin (DCX), a marker for immature neurons (Kempermann et al., 2004). We analyzed two neurogenic regions, the dentate gyrus (DG) of the hippocampus and the subventricular zone (SVZ; Kempermann et al., 2004).

In the DG, we observed a subtle but statistically not significant increase in DCX (Fig. 7B and F) and Nestin (Fig. 7D and H) positive cells upon FTY720 treatment compared to DMSO injected animals (Fig. 7A, E, C and G). In the SVZ, we observed DCX (Fig. 7I and M) and nestin (Fig. 7K and O) positive cells along the margins of the ventricle in DMSO treated mice. As seen for the hippocampus, FTY720 had overall a positive effect on neurogenesis in the SVZ. Now, the number of DCX positive neurons was significantly increased by FTY720 (Fig. 7J and N; quantified in S) and numbers of nestin positive cells were also slightly elevated (Fig. 7L and P; quantified in T).

Thus, our finding is congruent with recent data described for the DG (Efstathopoulos et al., 2015), indicating a positive role of FTY720 in neurogenesis.

3.5. FTY720 signaling is modulated by neuronal sphingosine receptors

To decipher which S1P receptors might be engaged by FTY720 on neurons, mRNA abundance of all five S1P receptors was quantified in primary cerebellar neurons (Fig. 8A). We observed highest expression of *S1pr3* and somewhat lower of *S1pr1* and *S1pr2*, whereas *S1pr4* and *S1pr5* where almost absent from these primary neurons (Fig. 8A).

It is known from the literature that FTY720 binds preferentially to S1PR1, S1PR3 and S1PR5 out of the five S1P receptors (Brunkhorst et al., 2014). In contrast, S1PR2 is not recognized by FTY720 (Brunkhorst et al., 2014). In order to decipher S1P receptors engaged by FTY720 we employed S1P receptor antagonists (Fig. 8B–J; see Fig. 11). This included the S1PR1 antagonist NIBR-0213, the S1PR2 antagonist JTE-013 and the S1PR3 antagonist TY52156 (Huwiler and Pfeilschifter, 2006; Murakami et al., 2010; Quancard et al., 2012).

As before (Fig. 1), FTY720 application alone for 24 h resulted in robust induction of all genes analyzed (Fig. 8B–J). Interestingly, co-application of FTY720 and the S1PR2 antagonist JTE-013 enhanced even further gene expression compared to FTY720 alone. This was observed for eight out of nine genes analyzed (Fig. 8B and D–J), the exception being *FosB* (Fig. 8C). This suggests that S1PR2 signaling inhibition potentiates FTY720's potential to induce neuronal gene expression. In contrast, NIBR-0213 co-administration resulted in a modest inhibition of several FTY720 induced genes including *Egr1* (Fig. 8D), *Egr2* (Fig. 8E), *Acta* (Fig. 8F), *Cnn1* (Fig. 8G), *Tagln* (Fig. 8H) and *Bdnf* (Fig. 8I) suggesting that FTY720 requires at least to some extent S1PR1 signaling. Interference with S1PR3 signaling by TY52156 administration had an opposite effect on FTY720 mediated IEG and cytoskeletal gene expression. Here, FTY720's potential to induce IEGs such as *c-Fos* (Fig. 8B) and *FosB* (Fig. 8C) was significantly further enhanced, as also seen for *Egr1* and *Egr2* (Fig. 8D and E). In opposite to this, FTY720 mediated mRNA induction of all three actin cytoskeletal (Fig. 8F–H) was significantly reduced by inhibition of S1PR3 receptors.

In contrast to FTY720, S1P did not generally induce gene expression with one exception, *Ccl2*. Here, S1P application resulted in strong *Ccl2* mRNA induction (Fig. 8J). Of note, this *Ccl2* induction appears completely

Fig. 4. FTY720 stimulates peripheral axon regeneration in vivo. (A) Experimental outline of the facial nerve lesion model. The facial nerve is represented by solid blue, dashed blue or red lines. The position of facial motoneurons in the *nucleus facialis* is labeled by a black dotted line. Time-line indicates FTY720 or DMSO injection every second day. Fluorogold (FG) tracer was injected 15 days after axotomy and animals were analyzed three days thereafter. (B–E) The *nucleus facialis* was stained with anti-FG directed antibodies to visualize the FG tracer. FTY720 treatment enhanced the number of FG positive motoneurons on the lesioned side (E) compared to DMSO injected animals (D). Individual FG tracer positive motoneurons are marked by arrows in D and E. (F–I) The number of motoneurons positive for the neurodegeneration marker SMI-32 was upregulated upon facial nerve lesion (H and I) compared to the unlesioned side (F and G). FTY720 injection (I) slightly reduced the number of SMI-32 positive neurons compared to control (H; see quantification in W). J–Q) IBA-positive microglial cells (J–M) and GFAP-positive astrocytes (N-Q) were comparably induced by facial nerve lesion in DMSO (L and P) and FTY720 (M and Q) treated animals compared to the unlesioned side (J and N; K and O). (R–U) Total numbers of facial motoneurons were labeled with Nissl. Numbers of motoneurons were slightly decreased upon lesion in both DMSO (T) and FTY720 (U) injected animals. (V) Quantification of axon regeneration. The number of regeneration-indicating tracer positive motoneurons was almost doubled upon FTY720 treatment. FG-positive neurons on the lesioned side were normalized to the numbers on the unlesioned side (set to 100%). (W) Quantification of SMI-32. The number of SMI-32 positive motoneurons on the lesioned side was decreased by approximately 20% upon FTY720 treatment, however, this result was statistically not significant (DMSO: 213 ± 19 neurons; FTY720: 177 ± 18 neurons; N = 7; P = 0.21). SMI-32 positive motoneurons on the unlesioned side were set to 100%. (X and Y) Microglia (X) and astrocytes (Y) were comparably induced in DMSO or FTY720 treated animals on the lesioned side. Numbers on the unlesioned side were set to 100%. (Z) Nissl positive motoneurons were reduced by approximately 10% upon lesion in both DMSO and FTY720 treated animals. Each circle or square represents one animal analyzed. The dashed line in (N–R) represents values obtained at the unlesioned side that were set to 100%. Data are expressed as mean ± SD. Scale-bar (B–U) = 100 μm.

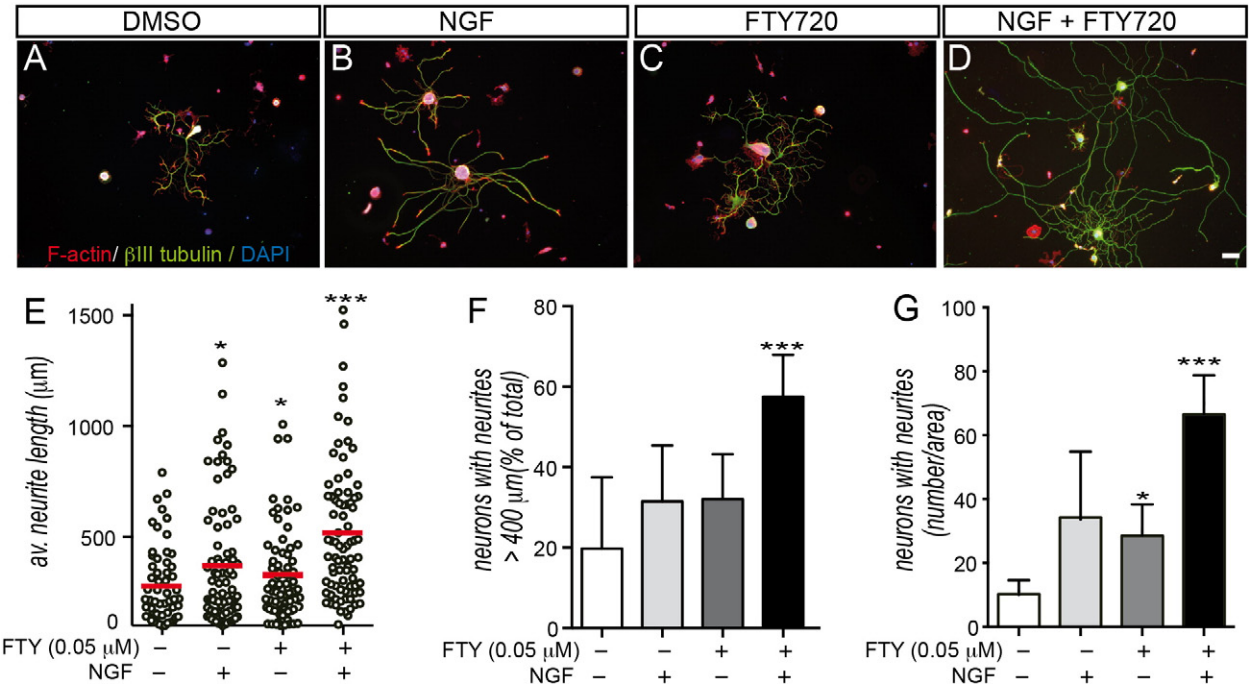

Fig. 5. FTY720 stimulates DRG neurite growth. (A–D) Adult mouse DRG neurons were incubated with NGF (B), FTY720 (C) or both together (D) and subsequently stained for neuron-specific βIII tubulin (green) and F-actin (red). NGF (B) and FTY720 (C) treatment alone stimulated DRG neurite growth. Combined treatment of NGF and FTY720 (D) even further enhanced neurite growth compared to control (A) and individual treatments of NGF or FTY720. (E–F) Quantification of DRG neurite growth by calculating average neurite length (E), the percentage of neurons with longest neurites (F) and number of neurons with neurite growth normalized to the area (G). Each circle in (E) represents one neuron. The red lines in (E) indicate the mean values. Statistical significance was calculated in relation to the DMSO treated control cultures (FTY "-"and NGF "-"). Scale-bar (A–D) = 50 μm.

dependent on S1PR2 receptors, as JTE-013 incubation almost completely abrogated *Ccl2* induction by S1P (Fig. 8J). This is in contrast to S1PR2's inhibitory impact on FTY720 signaling (see above).

We next analyzed whether S1PR inhibitors might also affect cerebellar neurite growth (Fig. 8K and L). Here, individual inhibition of S1PR1 and S1PR2 enhanced average neurite length (Fig. 8K) and the percentage of neurons bearing longest neurites (>40 μm; Fig. 8L). Inhibition of S1PR3 alone also enhanced neurite growth, however not significantly. Upon co-administration of FTY720 with S1PR inhibitors, only interference with S1PR1 resulted in decreased neurite growth (Fig. 8K and L). This suggests that FTY720 requires to some extent S1PR1 for signaling.

In summary, FTY720 stimulated neuronal gene expression and neurite growth is modulated by S1P receptor activity.

3.6. FTY720 recruits G12/13 G protein-RhoA-MRTF-A/SRF signaling in neurons

FTY720 recognizes S1P receptors, including those connected with G12/13 and RhoA signaling (Brinkmann et al., 2010; Brunkhorst et al., 2014). Activated RhoA-GTPase enhances nuclear activity of the transcription factor SRF and its cofactor MRTF-A. In order to analyze whether FTY720 triggers a neuronal signaling cascade through G12/13-RhoA-MRTF-A/SRF engagement, we employed specific blocking strategies for each of the signaling intermediates (Fig. 9). Overexpression of the RGS (regulator of G protein signaling) domain of the Rho-GTPase guanine nucleotide exchange factor (Rho-GEF) Lsc (Lsc-RGS) interferes with Gα12/13 signaling (Moepps et al., 2008). RhoA function was blocked by the C3 transferase (Barth et al., 1998) and MRTF-A was inhibited through overexpression of a dominant negative MRTF-A protein (Miralles et al., 2003). For a summary of blocking strategies see Fig. 11.

Inspection of the three IEG genes, *c-Fos* (Fig. 9A), *Egr1* (Fig. 9B) and *Egr2* (Fig. 9C) revealed induction of all three IEGs by FTY720 as before (Figs. 1 and 8). Inhibition of individual components of the G12/13-RhoA-MRTF-A pathway did not abrogate mRNA induction of all three IEGs (Fig. 9A–C). In fact, mRNA abundance of *c-Fos* or *Egr2* upon blocking individual components of the G12/13-RhoA-MRTF-A signaling pathway was actually augmented upon FTY720 administration (Fig. 9A and C).

In contrast, FTY720 required for induction of all three "actin genes", *i.e. Acta*, *Cnn* and *Tagln* an intact G12/13-RhoA-MRTF-A signaling pathway (Fig. 9D–F). For instance, FTY720 mediated upregulation of *Acta* was abrogated by inhibition of G12/13 G proteins, the RhoA-GTPase or MRTF-A gene transcription (Fig. 9D). The same holds true for *Tagln* (Fig. 9F) and to a weaker extent for *Cnn* (Fig. 9E). Data in Fig. 9D–F suggest that RhoA is involved in FTY720 signaling. We analyzed this further by inspecting whether downstream of RhoA, the known RhoA effector molecule cofilin (Bamburg et al., 2010), is involved in FTY720 signaling. For this, primary cerebellar neurons were stimulated with FTY720 for 1 h and protein lysates were subjected to immunoblotting with antibodies recognizing total cofilin and phosphorylated cofilin levels (Supplementary Fig. 4). Serine 3 phosphorylated cofilin represents the inactive form of this actin severing protein (Bamburg et al., 2010). Total cofilin protein abundance was not affected by FTY720 administration (Supplementary Fig. 4). In contrast, there was a subtle, but statistically not significant increase, in phosphorylated cofilin abundance by FTY720 application (Supplementary Fig. 4). This suggests a modest impact of FTY720 on cofilin activity.

Next, we asked whether neuronal signaling elicited by FTY720 targets SRF mediated gene transcription. For this, we performed qPCR experiments in primary cerebellar neurons focusing on the 24 h time point of FTY720 application (Fig. 10). In order to evaluate a potential SRF dependence of FTY720 action, we included siRNA mediated SRF downregulation. In addition, we analyzed siRNA mediated CREB downregulation, a transcription factor previously reported to be activated by FTY720 (Deogracias et al., 2012). Total SRF, total CREB

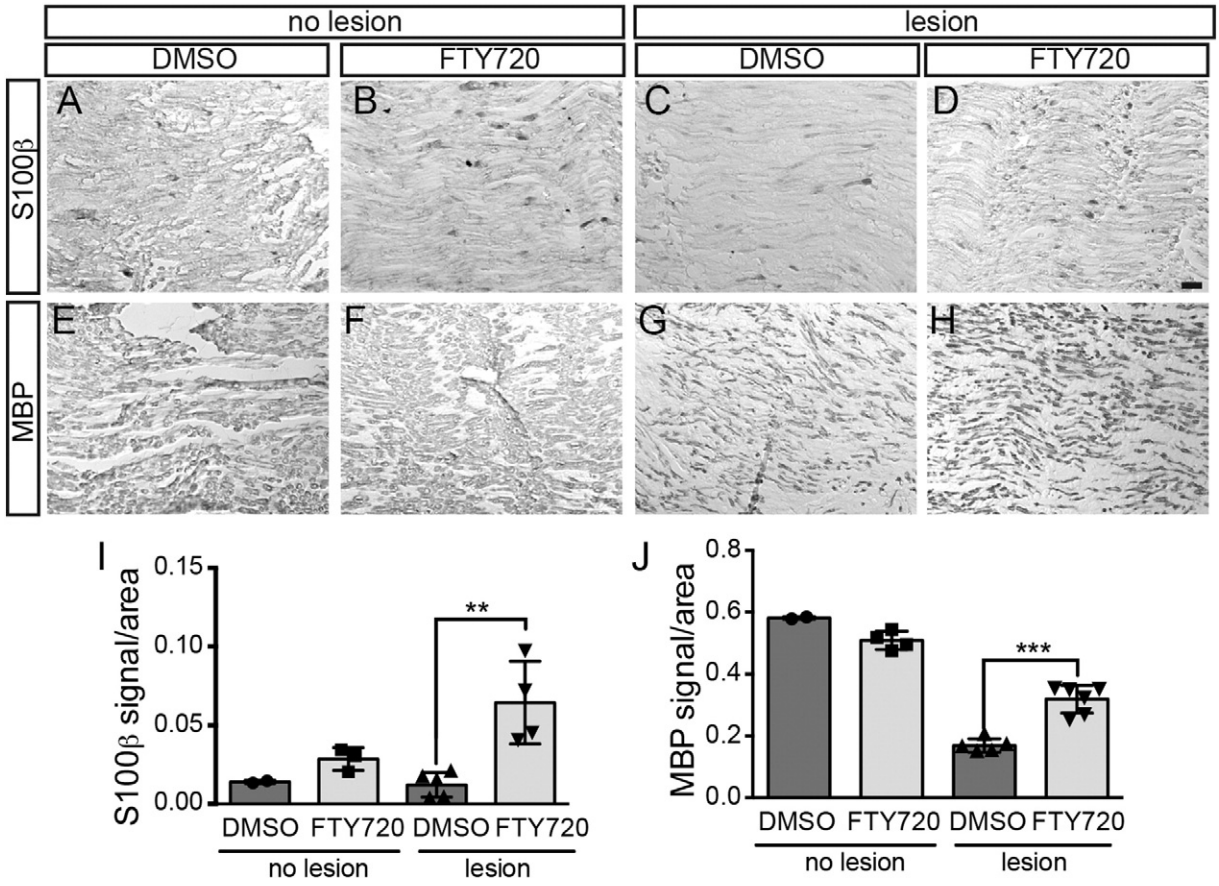

Fig. 6. FTY720 enhances Schwann cell signals and myelin content in lesioned nerves. Unlesioned and lesioned facial nerves of control or FTY720 treated mice were labeled for Schwann cells with S100β (A–D) or myelin with MBP (E-H) 18 days after injury. (A–D) Schwann cell signals were elevated in both unlesioned (B) and lesioned (D) facial nerves of FTY720 treated animals compared to control treated animals (A and C). (E–H) Upon injury, myelin content measured by MBP was elevated in FTY720 (H) compared to control treated animals (G). (I, J) Quantification of S100β (I) and MBP (J) signals per area. Each circle, triangle or square represents one animal analyzed. Data are represented as mean ± SD. Scale-bar (A-H) = 100 μm.

or activated P-CREB protein levels were clearly diminished by the respective *Srf* or *Creb* directed siRNA compared to a control siRNA (*siCtr.*; Fig. 10A).

In the presence of control siRNA, FTY720 induced *cFos* (Fig. 10B) and *FosB* (Fig. 10C) mRNA levels as before in non-electroporated neuronal cultures (Figs. 1 and 8). Upon siRNA mediated downregulation of SRF and CREB, FTY720 still induced *cFos* (Fig. 10B) and *FosB* (Fig. 10C) suggesting that this gene response is neither SRF nor CREB dependent. In contrast, FTY720 required the presence of SRF but not CREB for full induction of the IEGs *Egr1* (Fig. 10D) and *Egr2* (Fig. 10E).

Out of the four actin cytoskeletal genes tested, three, *i.e. Acta* (Fig. 10F), *Cnn* (Fig. 10H) and *Tagln* (Fig. 10I) but not *Tpm1a* (Fig. 10G) required SRF but not CREB for upregulation by FTY720. Finally, *Bdnf* (Fig. 10J) was upregulated by FTY720, however neither in an SRF- nor CREB-dependent manner. Expression of *Ccl2*, *Ccl3*, *Ccl9* chemokines and *S1pr1-5* receptors was not affected by siRNA mediated SRF depletion suggesting that expression of those genes is not SRF dependent (data not shown).

Taken together, FTY720 engages a G12/13-RhoA-MRTF-A/SRF signaling pathway in neurons to regulate actin cytoskeletal genes but not IEGs.

We also tested whether FTY720's impact on growth cone area and filopodia number requires SRF (Fig. 10K–P). In cerebellar neurons expressing control siRNAs (Fig. 8K and L), FTY720 elevated growth cone area and filopodia number as before (Fig. 3). In contrast, upon SRF depletion, FTY720 did not enhance growth cone area and filopodia number (Fig. 10M and N). This indicates an SRF dependence of FTY720 to modulate growth cone morphology (Fig. 10) and also neurite growth (data not shown).

4. Discussion

4.1. Neuronal functions of FTY720

In this study, we report direct modulation of neuronal function by FTY720. We observed two neuronal FTY720 activities, *i.e.* induction of a gene expression response (*e.g.* Figs. 1 and 8) and modulation of neuronal morphology, neurite growth and axonal regeneration (Figs. 3–5).

FTY720 increased mRNA abundance of several genes including IEGs (*c-Fos*, *FosB*, *Egr1*, *Egr2*, *Bdnf*), cytoskeletal genes and *Ccl2*. We identified with SRF a first transcription factor mediating such FTY720 gene induction in neurons (Fig. 10 and see below). Thus, similar to BDNF signaling (Chang et al., 2004; Kalita et al., 2006; Meier et al., 2011), SRF is also involved in FTY720 signaling. In addition to gene induction, FTY720 appears also to repress neuronal gene expression of *e.g. Ccl3* and *Ccl9* (Fig. 1), in line with a recent report in Schwann cells (Heinen et al., 2015).

What might be the functional consequences of such FTY720 upregulated gene products for neurons?

CCL chemokines mediate a brain intrinsic immune response involving astrocytes and microglia (Reaux-Le Goazigo et al., 2013). For instance, during PNS nerve injury CCL2 modulates Wallerian degeneration and

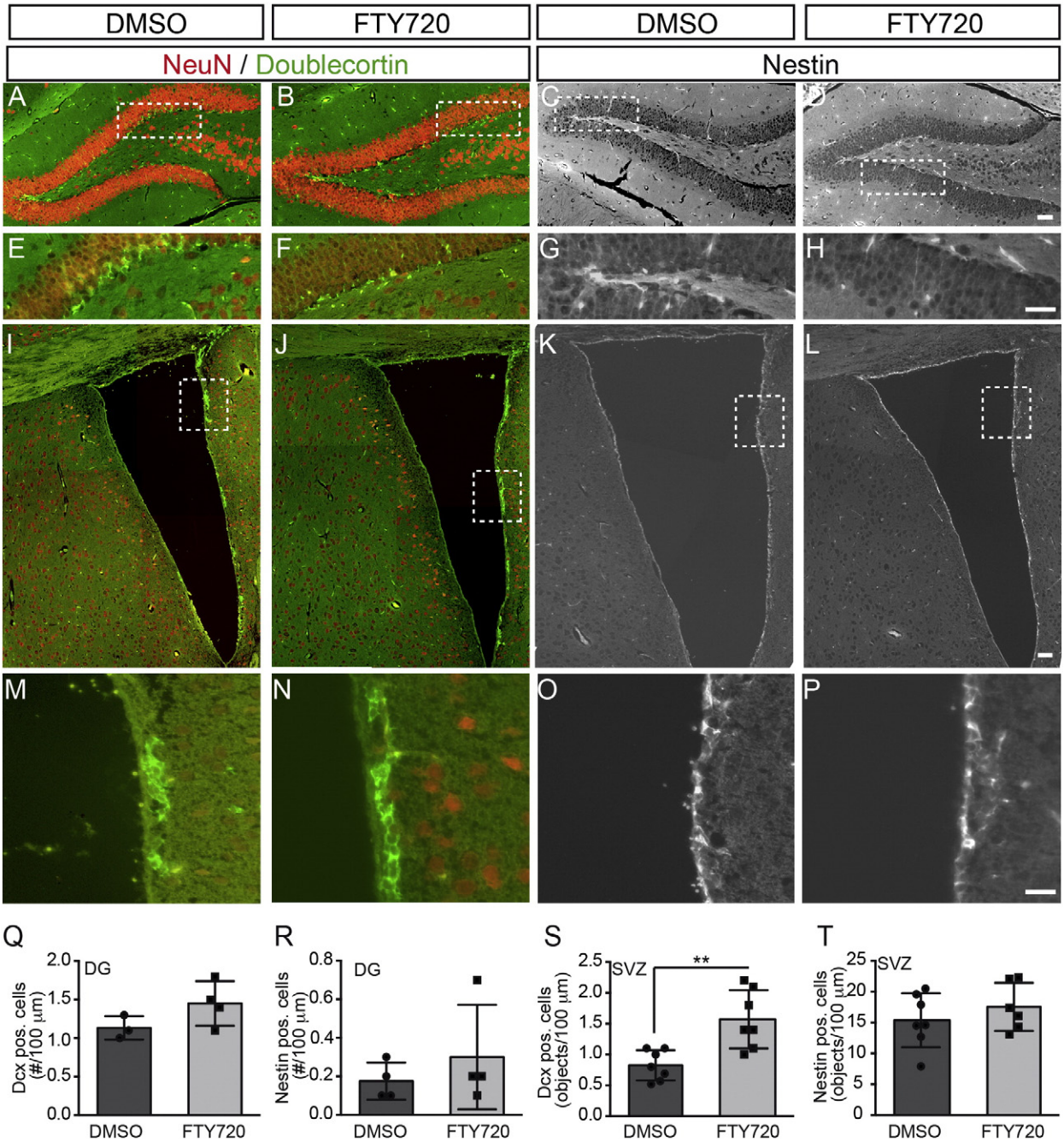

Fig. 7. FTY720's impact on hippocampal and SVZ neurogenesis. (A–H) The dentate gyrus (DG) of the hippocampus was stained for NeuN and doublecortin (DCX; A, B and E, F) or nestin (C, D and G, H) expression. DCX was found in the subgranular zone of the DG in both DMSO (A and E) and FTY720 (B and F) treated animals. Nestin positive cell bodies and protrusions were found in the DG of DMSO (C and G) and FTY720 (D and H) treated mice. (E–H) are higher magnifications of boxed areas in (A–D). (I–P) In the SVZ of control mice, DCX (I and M) and nestin (K and O) positive cells were found along the borders of the ventricle. FTY720 enhanced the number of DCX positive immature neurons (J and N; see S) and also slightly the number of nestin positive neurons (L and P; see T). (M–P) are higher magnifications of boxed areas in (I–L). (Q–T) Quantification of DCX (Q and S) or nestin (R and T) positive cells in the DG (Q and R) or SVZ (S and T). Overall, FTY720 enhanced signals for both neurogenesis markers in both regions, however statistically significantly only for DCX in the SVZ (S). Each circle or square represents one animal analyzed. Data are expressed as mean ± SD. Scale-bar (A–D; I–L) = 50 µm; (E–H; M–P) = 50 µm.

myelin debris clearance by regulation of macrophage responses (Perrin et al., 2005). Thus, through upregulation of CCL chemokines, FTY720 might influence Wallerian degeneration and myelin function during PNS axon regeneration (see also below).

FTY720 also induced several IEGs including *c-Fos*, *FosB*, *Egr1*, *Egr2* and *Bdnf* (Fig. 1). Interestingly, three genome-wide expression studies identified overrepresentation of IEGs such as *c-Fos* and *Egr1* in human MS patient tissue, suggesting important roles of these IEGs in MS pathogenesis (Kotelnikova et al., 2015; Liu et al., 2013; Riveros et al., 2010). Many of these IEGs encode for neuronal activity-induced and neuronal plasticity-associated transcription factors that are rapidly induced by neuronal activation. For instance, *c-Fos* induction is a *bona fide* marker to identify synaptically activated neurons. In turn, such IEGs elicit a second (delayed) gene transcription response modulating synaptic plasticity related properties of neuronal networks related to learning and memory (Perez-Cadahia et al., 2011). Thus, through governing a neuronal IEG response, FTY720 might directly regulate plasticity-related properties of neuronal circuits also in human MS patients (see summary

Fig. 11). Such beneficial FTY720 effects on learning and memory were recently reported in mice (Hait et al., 2014). In addition to modulation of synapse function, *c-Fos* and *Egr* transcription factors stimulate neurite growth *in vitro* (Levkovitz and Baraban, 2002; Levkovitz et al., 2001), axon sprouting *in vivo* (Watanabe et al., 1996) and are induced in some PNS lesion models (Herdegen et al., 1993; Herdegen and Leah, 1998). Thus, although we do not provide functional evidence in this study, it is reasonable to argue that FTY720 mediated upregulation of IEGs such as *c-Fos*, *Egr1* or *Egr2* might also modulate neurite growth *in vitro* and axon regeneration *in vivo*.

In addition to IEGs, FTY720 induced mRNA levels of genes encoding for components of the actin cytoskeleton such as *Acta*, calponin (*Cnn*), transgelin (*Tagln*) and tropomyosin (*Tpm1a*) family ABPs (Fig. 1). The actin cytoskeleton is an important regulator of neuronal growth cone dynamics and is also involved in stimulation of axon growth and regeneration (Bradke et al., 2012). In this study we observed that FTY720 upregulated several actin isoforms (Fig. 1). Interestingly, during several PNS injuries, including facial nerve axotomy (Tetzlaff and Bisby, 1990; Tetzlaff et al., 1988), an early but transient upregulation of actin levels was reported. Thus, FTY720 treatment might enhance abundance of actin isoforms during an early phase of axonal regeneration. In addition to actin isoforms, we observed induction of the ABPs calponin and tropomyosin by FTY720 (Fig. 1). These ABPs stabilize filopodial F-actin (Danninger and Gimona, 2000), enhance cell motility (Wu et al., 2014) and regulate neuritogenesis and growth cone shape (Curthoys et al., 2014; Pape et al., 2008; Schevzov et al., 2005). Thus, through induction of such specific ABPs FTY720 might exert a direct function on neuronal actin dynamics and thereby on growth cone shape and neurite growth.

In contrast to the actin cytoskeleton, we have not observed obvious effects of FTY720 on overall tubulin, tyrosinated or acetylated tubulin abundance (data not shown). FTY720's potential to influence the actin or ABP gene expression suggests modulation of actin-dependent processes such as neuronal morphology and motility. Indeed, FTY720 increased growth cone area and number of F-actin rich filopodia as well as neurite growth *in vitro* (Figs. 3 and 5) and axonal regeneration *in vivo* (Fig. 4). Thus, FTY720 appears to have positive effects on neuronal morphology and nerve fiber growth relying on actin cytoskeletal dynamics.

In contrast to FTY720, S1P was reported to induce growth cone collapse (Fincher et al., 2014; Strochlic et al., 2008) suggesting that FTY720 and S1P have opposite effects on neuronal morphology. Of note, FTY720 had a concentration-dependent effect on neurite growth with low and high concentrations stimulating or inhibiting neurite growth, respectively (Fig. 3E). Thus, similar to other treatments, *e.g.* ephrins (Hansen et al., 2004) and taxol employed in spinal cord injuries (Hellal et al., 2011), there might be a specific FTY720 concentration range beneficial for stimulating neuronal motility. We also noted, perhaps surprisingly, reduced growth cone shape and neurite growth upon co-application of FTY720 with BDNF, in contrast to individual application of either molecule in CNS neurons (Fig. 3). Currently, the implication of this counteraction remains unresolved, however a different neurotrophin, NT-3, was also reported to interfere with FTY720's impact on cells (Coelho et al., 2007). It is worth noting that in contrast to CNS neurons, co-application of FTY720 with a different neurotrophin, NGF, enhanced neurite growth in PNS neurons compared to individual application (Fig. 5).

Herein, we present first data demonstrating stimulation of axonal regeneration in the peripheral nervous system by FTY720 injection in mice (Fig. 4). In CNS spinal cord injury, FTY720 enhances functional recovery most likely through interfering with neuroinflammation (Lee et al., 2009). In this study, FTY720's beneficial impact on PNS axon regeneration most likely does not involve neuroinflammation, as judged by comparable microglia and astrocyte infiltration in the lesion side (Fig. 4). Our data favor direct stimulation of severed nerve fiber growth by FTY720 also *in vivo* (see summary Fig. 11). Indeed, FTY720 enhanced growth cone morphology and neurite growth of CNS neurons *in vitro* (Fig. 3). Besides CNS neurons, FTY720 alone or together with NGF also enhanced neurite growth of PNS neurons (Fig. 5). Interestingly, NGF, an established stimulator of PNS neurite growth, is strongly upregulated by facial nerve injury (Stern et al., 2012). Thus, such NGF upregulation upon facial nerve injury together with the injection of FTY720 might result in a concerted action of both molecules facilitating nerve growth and thereby PNS axonal regeneration. In line with such a pro-regenerative FTY720 function we observed FTY720 mediated induction of the neuroprotective RAG ATF3, also known to stimulate axon growth and regeneration (Supplementary Fig. 3; Seijffers et al., 2006, 2007).

In addition to axon growth, we observed that FTY720 enhanced Schwann cell numbers and abundance of MBP positive myelin in the injured facial nerve compared to control treated animals (Fig. 6). This is in line with previous reports showing FTY720's potential to stimulate a pro-regenerative Schwann cell phenotype (Heinen et al., 2015) and augment MBP expression during remyelination (Jackson et al., 2011). This suggests that FTY720 might enhance facial nerve regeneration also through modulation of Schwann cell function.

4.2. How might FTY720 modulate neuronal signaling?

FTY720 can modulate signaling, *e.g.* epigenetic modifications, through a direct nuclear localization (Hait et al., 2014). In addition, FTY720 acts at the cell surface as a S1P receptor agonist or, upon prolonged treatment, as antagonist through S1PR internalization (Chun and Brinkmann, 2011). Our data suggest that FTY720 mediates a signaling cascade modulated by S1P receptors. First of all, we observed neuronal expression of S1P receptors known to be engaged by FTY720 (*i.e.* S1PR1 and S1PR3 as also reported by others; Deogracias et al., 2012; Kays et al., 2012). Pharmacological interference with S1PR1 receptors revealed a subtle dependence of FTY720 signaling on this receptor for gene expression and neurite growth (Fig. 8). Strikingly however, S1PR2 inhibition with the antagonist JTE-013, augmented FTY720's individual activity on gene expression in primary neurons (Fig. 8). This suggests that S1PR2 receptor signaling, a receptor actually not recognized by FTY720 (Chun and Brinkmann, 2011), counteracts FTY720 activity by so far unknown mechanisms. Notably, such co-application of FTY720 along with JTE-013 might be exploited to further enhance FTY720's individual activity, a finding with potential therapeutic relevance. In fact, JTE-013 was recently shown to enhance the neurite growth and regeneration potential of primary neurons (Kempf et al., 2014).

Finally, we show that inhibition of S1PR3 signaling had a dual effect on FTY720 mediated gene expression. S1PR3 receptor seems to inhibit FTY720's potential to induce IEGs, whereas this receptor was required by FTY720 for full induction of cytoskeletal genes (Fig. 8).

Downstream of S1P receptors, we demonstrate that FTY720 signaling targets the transcription factor SRF. Indeed, siRNA mediated SRF knockdown revealed that most of the genes induced by FTY720 required SRF except for *c-Fos* and *FosB* (Fig. 10). We further deciphered potential signaling intermediates between FTY720 and SRF and identified G12/13, RhoA and MRTF-A as potential candidates (Fig. 9 and summary Fig. 11). Both, G12/13 and RhoA are known MRTF-A/SRF activators (Mao et al., 1998; Olson and Nordheim, 2010). Of note, this G12/13-RhoA-MRTF-A/SRF signaling cascade was mainly involved in mediating FTY720's activity on cytoskeletal but not IEG gene expression and (Fig. 9 and summary Fig. 11), a finding congruent with previous data in neuronal and non-neuronal cells (Olson and Nordheim, 2010). With regard to IEG induction, our data suggest that FTY720 also requires SRF, however, this time SRF might cooperate with different cofactors, *e.g.* members of the TCF family (Knoll and Nordheim, 2009).

In summary, SRF is an important regulator of neuronal actin dynamics (Knoll and Nordheim, 2009; Olson and Nordheim, 2010) and stimulates axon growth and regeneration *in vivo* (Knoll et al., 2006; Lu and Ramanan, 2011; Stern et al., 2013; Wickramasinghe et al., 2008). Thus,

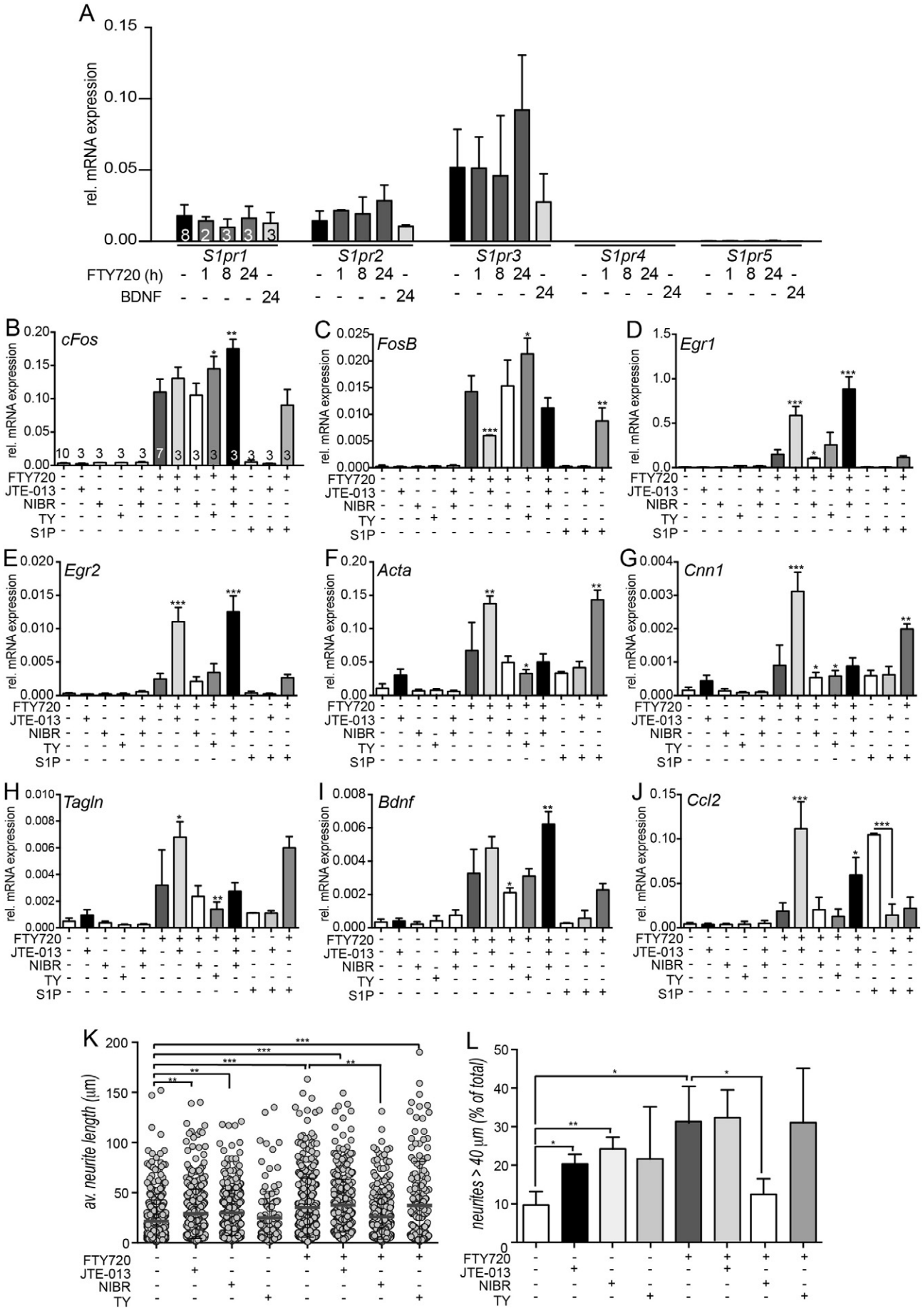
A
rel. mRNA expression
S1pr1
S1pr2
S1pr3
S1pr4
S1pr5
FTY720 (h)
BDNF
B cFos
C FosB
D Egr1
E Egr2
F Acta
G Cnn1
H Tagln
I Bdnf
J Ccl2
FTY720
JTE-013
NIBR
TY
S1P
K av. neurite length (µm)
L neurites > 40 µm (% of total)

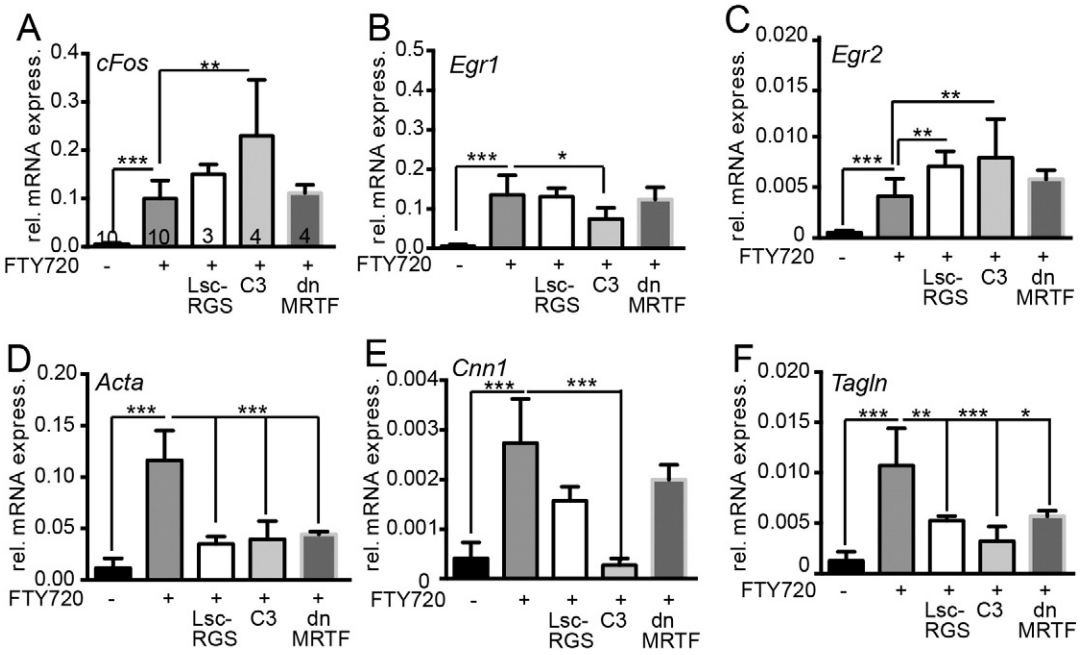

Fig. 9. FTY720 modulates gene expression through a G12/13-RhoA-MRTF-A cascade. (A–F) Cerebellar neurons were stimulated with FTY720 in the presence or absence of selective pathway inhibitors. Overexpression of Lsc-RGS or dominant-negative (dn) MRTF-A inhibits G12/13 and the SRF cofactor MRTF-A, respectively. Bath application of the C3 toxin specifically interferes with RhoA-GTPase activity. Subsequently, qPCR experiments were performed, depicting relative mRNA levels of *cFos* (A), *Egr1* (B) or *Egr2* (C) upon the various treatments indicated. (A–C) In the absence of pathway blocking agents, FTY720 robustly augmented mRNA levels of all three IEGs. In comparison to FTY720 alone, blocking G12/13 and RhoA signaling further elevated mRNA abundance of *cFos* (A) and *Egr2* (C) but not *Egr1* (B). In contrast, blocking MRTF-A did not modulate FTY720's induction of all three IEGs. (D–F) Blocking of all three signaling intermediates, G12/13, RhoA and MRTF-A, prevented induction of all three actin cytoskeletal genes, *Acta* (D), *Cnn* (E) and *Tagln* (F) by FTY720. Numbers in bars in (A) indicate the number of independent cell cultures analyzed for each gene depicted. Data are expressed as mean ± SD.

through connecting with SRF, FTY720 might have direct access to actin cytoskeleton based processes such as modulation of growth cone shape and axon growth and re-growth after injury.

4.3. Implications for treatment of MS and other neurological diseases

Enhancing neuroprotection is a goal shared by many therapeutic efforts to cure neurodegenerative diseases. In recent years, several molecules have been attributed neuroprotective effects in animal models of neurodegenerative diseases. For instance, melanocortins prevent cognitive decline in mouse models of Alzheimer's disease (Giuliani et al., 2011, 2014, 2015). Melancortins might exert their neuroprotective activity through enhancing neurogenesis (Giuliani et al., 2011, 2014, 2015), a function also reported for FTY720 (Fig. 7 and Efstathopoulos et al., 2015).

In this study, we identified FTY720 as a potential candidate providing neuroprotection in neurological diseases including – but not limited to – MS. In latest MS research, the neuronal compartment has been assigned an important role at early stages of MS pathology. Now, axonal damage and neurodegeneration are viewed as a prime MS cause (Luessi et al., 2012; Trapp and Nave, 2008). Thus, stressing the importance of neurodegeneration in MS in addition to inflammation has significant implications for treatment strategies. In this regard, it might be particularly important to stimulate neuroprotective and neuroregenerative processes of damaged neurons in MS therapy. In this study, we showed such FTY720 mediated neuroprotective and neurorestorative functions directly on CNS neurons. FTY720's potential to elicit neuronal activity associated gene expression as well as modulation of actin dependent growth cone shape, neurite growth and axonal regeneration might enhance neuroprotective processes in MS affected CNS neurons and dampen MS associated neuronal impairments including synaptopathies, axonal damage and neuronal demise.

In addition, our data suggest that FTY720 treatment might also be beneficial for treatment of other neurological diseases including central and peripheral nerve injuries requiring improvement of neuroprotective or neuroregenerative processes.

5. Conclusions

FTY720 (FTY720) is now a routinely employed drug to treat multiple sclerosis. So far, FTY720's mode of action was believed to mainly involve sequestration of auto-reactive immune cells in lymph nodes. In this study, we demonstrate that FTY720 has direct actions on neurons including stimulation of a neuronal-plasticity associated gene expression response, nerve fiber growth and axonal regeneration of lesioned nerves

Fig. 8. FTY720 mediated gene expression is modulated by S1P receptor antagonists. (A) Primary cerebellar neurons were incubated with FTY720 or BDNF for timepoints indicated and subsequently cDNA was subjected to qPCR analysis with S1P receptor primer pairs as indicated. Out of the five S1P receptors, *S1pr3* mRNA abundance was strongest, *S1pr1* and *S1pr2* were weaker expressed and *S1pr4* and *S1pr5* were not expressed at all. Treatment with FTY720 or BDNF did not obviously affect mRNA abundance of *S1pr1-5*. (B–J) Primary cerebellar neurons were stimulated for 24 h with FTY720 or S1P in the presence or absence of specific S1PR1 (NIBR), S1PR2 (JTE-013) and S1PR3 (TY-52156) antagonists. Subsequently, mRNA levels of genes indicated were determined. FTY720 treatment alone stimulated mRNA abundance of all genes analyzed. Co-application of FTY720 with JTE-013 resulted in further augmentation of mRNA induction in almost all genes analyzed, except for *FosB* (C). NIBR co-application, in contrast, resulted in a slight inhibition of FTY720 mediated gene induction (see *e.g.* D, F, G, H and I). Interference with S1PR3 signaling further enhanced FTY720's potential to induce IEGs (B-E), whereas cytoskeletal gene expression was reduced (F-H). S1P administration induced gene expression only of one single gene, namely induction of *Ccl2* (J). Co-application of S1P with JTE-013 ablated this S1P mediated gene induction (J) in contrast to JTE-013's stimulatory impact on FTY720 (see above). (K and L) Quantification of average cerebellar neurite length (K) or percentage of neurons with longest neurites (L) upon the different treatments. Each circle in (K) represents one neuron. The red lines in (K) indicate the mean values. Numbers in (B) indicate independent cultures analyzed. Statistical significance was determined in relation to FTY720 treatment alone, if not indicated otherwise. Data are expressed as mean ± SD.

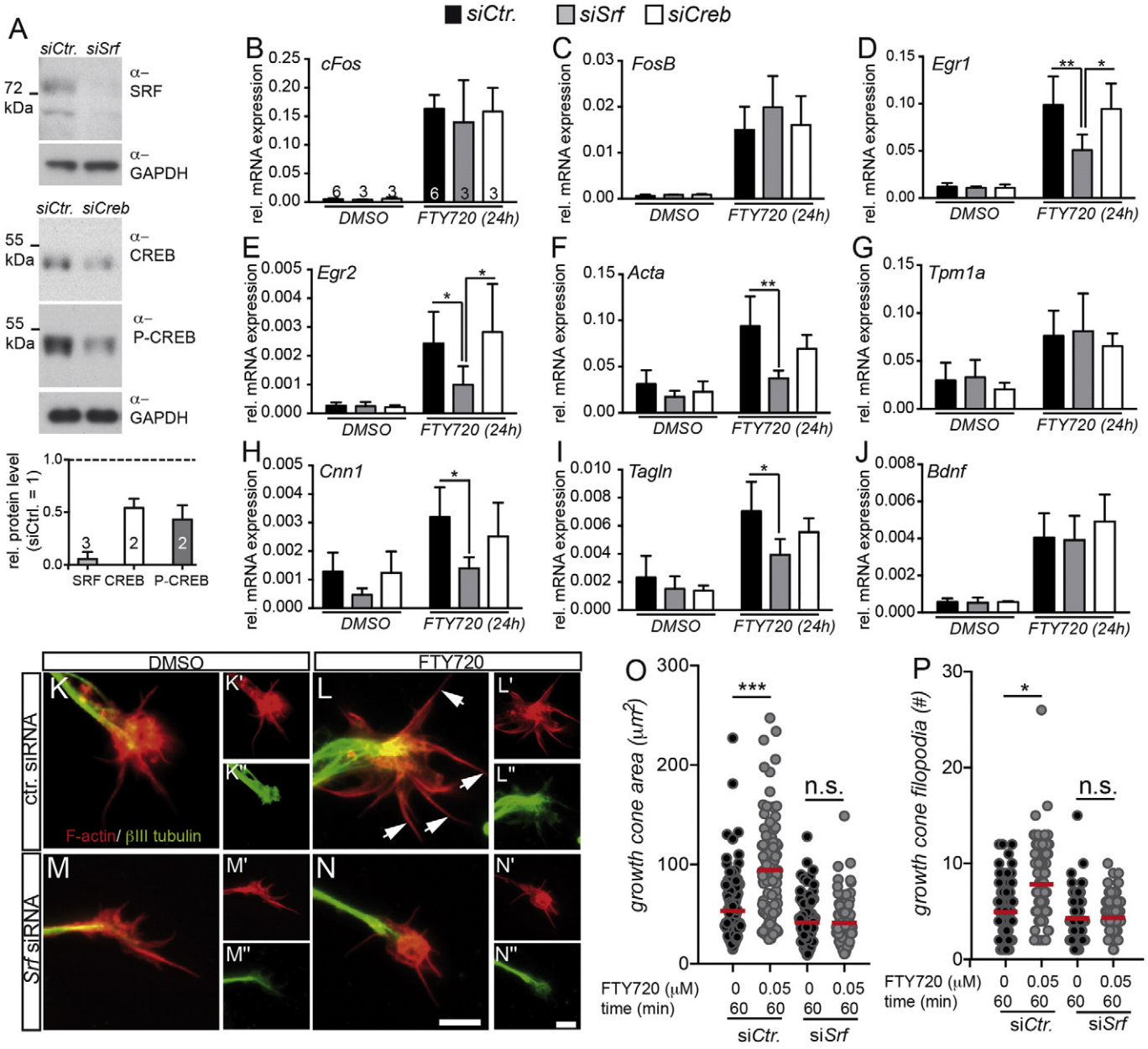

Fig. 10. FTY720 activity requires the gene regulator SRF. Cerebellar neurons were electroporated with control siRNA (*siCtr.*) or siRNA targeting either SRF (*siSrf*) or CREB (*siCreb*). Subsequently, neurons were incubated with DMSO or FTY720 for times indicated, followed by qPCR analysis for genes indicated (B-J) or by labeling growth cones for F-actin (red) and βIII tubulin (green; K–P). (A) Immunoblotting experiments demonstrating efficacy of siRNAs employed. *Srf* directed siRNA resulted in SRF downregulation, whereas siRNA directed against *Creb* resulted in downregulation of total CREB and activated CREB (P-CREB). For quantification, *siCtr.* levels were set to 1. (B–J) Upon SRF reduction, FTY720 mediated induction of gene transcription of *Egr1*, *Egr2*, *Acta*, *Cnn* and *Tagln* but not of *cFos*, *FosB*, *Tpm1a* or *Bdnf* was reduced. In contrast, induction of all genes by FTY720 was still possible upon CREB downregulation. Numbers in bars in (B) indicate the number of independent cell cultures analyzed for each gene depicted in (B–J). (K) Growth cone of a DMSO treated neuron electroporated with control siRNA. (K–K″) are individual channels depicting F-actin and βIII tubulin localization, respectively. (L) FTY720 application to the culture medium enhanced growth cone area and filopodia number (arrows) of a neuron treated with control siRNA. (M) The growth cone of a neuron with SRF downregulation consisted of a slightly smaller growth cone area with fewer filopodia. (N) FTY720 failed to enhance growth cone area and filopodia number of a neuron with SRF downregulation. (O and P) Quantification of growth cone area (O; in μm^2) or number of filopodia/growth cone (P) for the different conditions. Each individual circle represents a single growth cone derived from one of at least three independent experiments. Statistical significance was calculated in relation to the DMSO treated control cultures (0 μM FTY720). The red lines indicate the mean values. Scale-bar (K–N) = 5 μm; (K′–N′; K″–N″) = 5 μm.

in vivo. Thus, our data suggest that during MS therapy, FTY720 might also target neurons and might be beneficial to enhance neuroprotective and neurorestorative processes. In addition, our data suggest that FTY720 treatment might also be beneficial for treatment of other neurodegenerative diseases as well as central and peripheral nerve injuries.

Abbreviations

BDNF	brain derived neurotrophic factor
IEG	immediate early gene
MRTF	myocardin related transcription factor
MS	multiple sclerosis
NGF	nerve growth factor
RAG	regeneration associated gene
SRF	serum response factor
S1P	sphingosine-1-phosphate

Competing interests

The authors declare no conflict of interest.

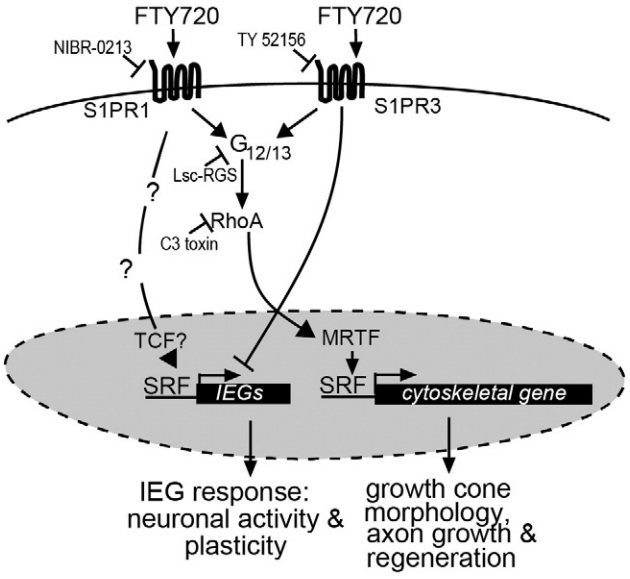

Fig. 11. Summary of FTY720's activity on neurons. FTY720 elicits in neurons an IEG response connected to neuronal activity mediated gene transcription. In addition, FTY720 was able to induce an actin cytoskeletal gene response associated with altered growth cone morphology, enhanced neurite growth and axon regeneration. FTY720 signaling depends partially on S1PR1 and S1PR3 receptors. In contrast, S1PR2 receptors appear to block FTY720 activity. FTY720's activity on the actin cytoskeleton is mediated through a G12/13-RhoA-MRTF-A/SRF dependent signaling cascade. FTY720 mediated IEG upregulation requires different signaling intermediates including SRF and potentially SRF cofactors of the TCF family. The scheme also lists inhibitory agents employed in this study.

Authors' contribution

SA performed all the experiments. BK analyzed the experiments, designed the study and wrote the manuscript.

Acknowledgements

B.K. is supported by the DFG (Deutsche Forschungsgemeinschaft) (D.4923) through the SFB 1149, Schram, Gottschalk and Gemeinnützige Hertie Foundation. We thank Daniela Sinske for her technical support.

Appendix A. Supplementary data

Supplementary data to this article can be found online at http://dx.doi.org/10.1016/j.expneurol.2016.03.012.

References

Alberti, S., Krause, S.M., Kretz, O., Philippar, U., Lemberger, T., Casanova, E., Wiebel, F.F., Schwarz, H., Frotscher, M., Schutz, G., Nordheim, A., 2005. Neuronal migration in the murine rostral migratory stream requires serum response factor. Proc. Natl. Acad. Sci. U. S. A. 102, 6148–6153.

Anastasiadou, S., Liebenehm, S., Sinske, D., Meyer zu Reckendorf, C., Moepps, B., Nordheim, A., Knoll, B., 2015. Neuronal expression of the transcription factor serum response factor modulates myelination in a mouse multiple sclerosis model. Glia 63, 958–976.

Bamburg, J.R., Bernstein, B.W., Davis, R.C., Flynn, K.C., Goldsbury, C., Jensen, J.R., Maloney, M.T., Marsden, I.T., Minamide, L.S., Pak, C.W., Shaw, A.E., Whiteman, I., Wiggan, O., 2010. ADF/cofilin-actin rods in neurodegenerative diseases. Curr. Alzheimer Res. 7, 241–250.

Barth, H., Hofmann, F., Olenik, C., Just, I., Aktories, K., 1998. The N-terminal part of the enzyme component (C2I) of the binary Clostridium botulinum C2 toxin interacts with the binding component C2II and functions as a carrier system for a Rho ADP-ribosylating C3-like fusion toxin. Infect. Immun. 66, 1364–1369.

Beck, H., Flynn, K., Lindenberg, K.S., Schwarz, H., Bradke, F., Di Giovanni, S., Knoll, B., 2012. Serum Response Factor (SRF)-cofilin-actin signaling axis modulates mitochondrial dynamics. Proc. Natl. Acad. Sci. U. S. A. 109, E2523–E2532.

Blanc, C.A., Rosen, H., Lane, T.E., 2014. FTY720 (fingolimod) modulates the severity of viral-induced encephalomyelitis and demyelination. J. Neuroinflammation 11, 138.

Bose, S., Cho, J., 2013. Role of chemokine CCL2 and its receptor CCR2 in neurodegenerative diseases. Arch. Pharm. Res. 36, 1039–1050.

Bradke, F., Fawcett, J.W., Spira, M.E., 2012. Assembly of a new growth cone after axotomy: the precursor to axon regeneration. Nat. Rev. Neurosci. 13, 183–193.

Brinkmann, V., Billich, A., Baumruker, T., Heining, P., Schmouder, R., Francis, G., Aradhye, S., Burtin, P., 2010. Fingolimod (FTY720): discovery and development of an oral drug to treat multiple sclerosis. Nat. Rev. Drug Discov. 9, 883–897.

Brunkhorst, R., Vutukuri, R., Pfeilschifter, W., 2014. Fingolimod for the treatment of neurological diseases-state of play and future perspectives. Front. Cell. Neurosci. 8, 283.

Chang, S.H., Poser, S., Xia, Z., 2004. A novel role for serum response factor in neuronal survival. J. Neurosci. 24, 2277–2285.

Choi, J.W., Gardell, S.E., Herr, D.R., Rivera, R., Lee, C.W., Noguchi, K., Teo, S.T., Yung, Y.C., Lu, M., Kennedy, G., Chun, J., 2011. FTY720 (fingolimod) efficacy in an animal model of multiple sclerosis requires astrocyte sphingosine 1-phosphate receptor 1 (S1P1) modulation. Proc. Natl. Acad. Sci. U. S. A. 108, 751–756.

Chun, J., Brinkmann, V., 2011. A mechanistically novel, first oral therapy for multiple sclerosis: the development of fingolimod (FTY720, gilenya). Discov. Med. 12, 213–228.

Chun, J., Hartung, H.P., 2010. Mechanism of action of oral fingolimod (FTY720) in multiple sclerosis. Clin. Neuropharmacol. 33, 91–101.

Coelho, R.P., Payne, S.G., Bittman, R., Spiegel, S., Sato-Bigbee, C., 2007. The immunomodulator FTY720 has a direct cytoprotective effect in oligodendrocyte progenitors. J. Pharmacol. Exp. Ther. 323, 626–635.

Cui, Q.L., Fang, J., Kennedy, T.E., Almazan, G., Antel, J.P., 2014. Role of p38MAPK in S1P receptor-mediated differentiation of human oligodendrocyte progenitors. Glia 62, 1361–1375.

Curthoys, N.M., Freittag, H., Connor, A., Desouza, M., Brettle, M., Poljak, A., Hall, A., Hardeman, E., Schevzov, G., Gunning, P.W., Fath, T., 2014. Tropomyosins induce neuritogenesis and determine neurite branching patterns in B35 neuroblastoma cells. Mol. Cell. Neurosci. 58, 11–21.

Danninger, C., Gimona, M., 2000. Live dynamics of GFP-calponin: isoform-specific modulation of the actin cytoskeleton and autoregulation by C-terminal sequences. J. Cell Sci. 113 (Pt 21), 3725–3736.

Deogracias, R., Yazdani, M., Dekkers, M.P., Guy, J., Ionescu, M.C., Vogt, K.E., Barde, Y.A., 2012. Fingolimod, a sphingosine-1 phosphate receptor modulator, increases BDNF levels and improves symptoms of a mouse model of Rett syndrome. Proc. Natl. Acad. Sci. U. S. A. 109, 14230–14235.

Di Menna, L., Molinaro, G., Di Nuzzo, L., Riozzi, B., Zappulla, C., Pozzilli, C., Turrini, R., Caraci, F., Copani, A., Battaglia, G., Nicoletti, F., Bruno, V., 2013. Fingolimod protects cultured cortical neurons against excitotoxic death. Pharmacol. Res. 67, 1–9.

Efstathopoulos, P., Kourgiantaki, A., Karali, K., Sidiropoulou, K., Margioris, A.N., Gravanis, A., Charalampopoulos, I., 2015. Fingolimod induces neurogenesis in adult mouse hippocampus and improves contextual fear memory. Transl. Psychiatry 5, e685.

Fincher, J., Whiteneck, C., Birgbauer, E., 2014. G-protein-coupled receptor cell signaling pathways mediating embryonic chick retinal growth cone collapse induced by lysophosphatidic acid and sphingosine-1-phosphate. Dev. Neurosci. 36, 443–453.

Flynn, K.C., Hellal, F., Neukirchen, D., Jacob, S., Tahirovic, S., Dupraz, S., Stern, S., Garvalov, B.K., Gurniak, C., Shaw, A.E., Meyn, L., Wedlich-Soldner, R., Bamburg, J.R., Small, J.V., Witke, W., Bradke, F., 2012. ADF/cofilin-mediated actin retrograde flow directs neurite formation in the developing brain. Neuron 76, 1091–1107.

Fox, R.J., Kita, M., Cohan, S.L., Henson, L.J., Zambrano, J., Scannevin, R.H., O'Gorman, J., Novas, M., Dawson, K.T., Phillips, J.T., 2014. BG-12 (dimethyl fumarate): a review of mechanism of action, efficacy, and safety. Curr. Med. Res. Opin. 30, 251–262.

Giuliani, D., Galantucci, M., Neri, L., Canalini, F., Calevro, A., Bitto, A., Ottani, A., Vandini, E., Sena, P., Sandrini, M., Squadrito, F., Zaffe, D., Guarini, S., 2014. Melanocortins protect against brain damage and counteract cognitive decline in a transgenic mouse model of moderate Alzheimers disease. Eur. J. Pharmacol. 740, 144–150.

Giuliani, D., Neri, L., Canalini, F., Calevro, A., Ottani, A., Vandini, E., Sena, P., Zaffe, D., Guarini, S., 2015. NDP-alpha-MSH induces intense neurogenesis and cognitive recovery in Alzheimer transgenic mice through activation of melanocortin MC4 receptors. Mol. Cell. Neurosci. 67, 13–21.

Giuliani, D., Zaffe, D., Ottani, A., Spaccapelo, L., Galantucci, M., Minutoli, L., Bitto, A., Irrera, N., Contri, M., Altavilla, D., Botticelli, A.R., Squadrito, F., Guarini, S., 2011. Treatment of cerebral ischemia with melanocortins acting at MC4 receptors induces marked neurogenesis and long-lasting functional recovery. Acta Neuropathol. 122, 443–453.

Hait, N.C., Wise, L.E., Allegood, J.C., O'Brien, M., Avni, D., Reeves, T.M., Knapp, P.E., Lu, J., Luo, C., Miles, M.F., Milstien, S., Lichtman, A.H., Spiegel, S., 2014. Active, phosphorylated fingolimod inhibits histone deacetylases and facilitates fear extinction memory. Nat. Neurosci. 17, 971–980.

Hansen, M.J., Dallal, G.E., Flanagan, J.G., 2004. Retinal axon response to ephrin-as shows a graded, concentration-dependent transition from growth promotion to inhibition. Neuron 42, 717–730.

Hasegawa, Y., Suzuki, H., Sozen, T., Rolland, W., Zhang, J.H., 2010. Activation of sphingosine 1-phosphate receptor-1 by FTY720 is neuroprotective after ischemic stroke in rats. Stroke 41, 368–374.

Heinen, A., Beyer, F., Tzekova, N., Hartung, H.P., Kury, P., 2015. Fingolimod induces the transition to a nerve regeneration promoting Schwann cell phenotype. Exp. Neurol. 271, 25–35.

Hellal, F., Hurtado, A., Ruschel, J., Flynn, K.C., Laskowski, C.J., Umlauf, M., Kapitein, L.C., Strikis, D., Lemmon, V., Bixby, J., Hoogenraad, C.C., Bradke, F., 2011. Microtubule stabilization reduces scarring and causes axon regeneration after spinal cord injury. Science 331, 928–931.

Herdegen, T., Kiessling, M., Bele, S., Bravo, R., Zimmermann, M., Gass, P., 1993. The KROX-20 transcription factor in the rat central and peripheral nervous systems: novel

expression pattern of an immediate early gene-encoded protein. Neuroscience 57, 41–52.
Herdegen, T., Leah, J.D., 1998. Inducible and constitutive transcription factors in the mammalian nervous system: control of gene expression by Jun, Fos and Krox, and CREB/ATF proteins. Brain Res. Brain Res. Rev. 28, 370–490.
Hunt, D., Raivich, G., Anderson, P.N., 2012. Activating transcription factor 3 and the nervous system. Front. Mol. Neurosci. 5, 7.
Huwiler, A., Pfeilschifter, J., 2006. Altering the sphingosine-1-phosphate/ceramide balance: a promising approach for tumor therapy. Curr. Pharm. Des. 12, 4625–4635.
Ingwersen, J., Aktas, O., Kuery, P., Kieseier, B., Boyko, A., Hartung, H.P., 2012. Fingolimod in multiple sclerosis: mechanisms of action and clinical efficacy. Clin. Immunol. 142, 15–24.
Jackson, S.J., Giovannoni, G., Baker, D., 2011. Fingolimod modulates microglial activation to augment markers of remyelination. J. Neuroinflammation 8, 76.
Kalita, K., Kharebava, G., Zheng, J.J., Hetman, M., 2006. Role of megakaryoblastic acute leukemia-1 in ERK1/2-dependent stimulation of serum response factor-driven transcription by BDNF or increased synaptic activity. J. Neurosci. 26, 10020–10032.
Kays, J.S., Li, C., Nicol, G.D., 2012. Expression of sphingosine 1-phosphate receptors in the rat dorsal root ganglia and defined single isolated sensory neurons. Physiol. Genomics 44, 889–901.
Kempermann, G., Jessberger, S., Steiner, B., Kronenberg, G., 2004. Milestones of neuronal development in the adult hippocampus. Trends Neurosci. 27, 447–452.
Kempf, A., Tews, B., Arzt, M.E., Weinmann, O., Obermair, F.J., Pernet, V., Zagrebelsky, M., Delekate, A., Iobbi, C., Zemmar, A., Ristic, Z., Gullo, M., Spies, P., Dodd, D., Gygax, D., Korte, M., Schwab, M.E., 2014. The sphingolipid receptor S1PR2 is a receptor for Nogo-a repressing synaptic plasticity. PLoS Biol. 12, e1001763.
Kim, H.J., Miron, V.E., Dukala, D., Proia, R.L., Ludwin, S.K., Traka, M., Antel, J.P., Soliven, B., 2011. Neurobiological effects of sphingosine 1-phosphate receptor modulation in the cuprizone model. FASEB J. 25, 1509–1518.
Knoll, B., Kretz, O., Fiedler, C., Alberti, S., Schutz, G., Frotscher, M., Nordheim, A., 2006. Serum response factor controls neuronal circuit assembly in the hippocampus. Nat. Neurosci. 9, 195–204.
Knoll, B., Nordheim, A., 2009. Functional versatility of transcription factors in the nervous system: the SRF paradigm. Trends Neurosci. 32, 432–442.
Kotelnikova, E., Bernardo-Faura, M., Silberberg, G., Kiani, N.A., Messinis, D., Melas, I.N., Artigas, L., Schwartz, E., Mazo, I., Masso, M., Alexopoulos, L.G., Mas, J.M., Olsson, T., Tegner, J., Martin, R., Zamora, A., Paul, F., Saez-Rodriguez, J., Villoslada, P., 2015. Signaling networks in MS: a systems-based approach to developing new pharmacological therapies. Mult. Scler. 21, 138–146.
Laskawi, R., Wolff, J.R., 1996. Changes in the phosphorylation of neurofilament proteins in facial motoneurons following various types of nerve lesion. ORL J. Otorhinolaryngol. Relat. Spec. 58, 13–22.
Lee, K.D., Chow, W.N., Sato-Bigbee, C., Graf, M.R., Graham, R.S., Colello, R.J., Young, H.F., Mathern, B.E., 2009. FTY720 reduces inflammation and promotes functional recovery after spinal cord injury. J. Neurotrauma 26, 2335–2344.
Levkovitz, Y., Baraban, J.M., 2002. A dominant negative Egr inhibitor blocks nerve growth factor-induced neurite outgrowth by suppressing c-Jun activation: role of an Egr/c-Jun complex. J. Neurosci. 22, 3845–3854.
Levkovitz, Y., O'Donovan, K.J., Baraban, J.M., 2001. Blockade of NGF-induced neurite outgrowth by a dominant-negative inhibitor of the egr family of transcription regulatory factors. J. Neurosci. 21, 45–52.
Liu, M., Hou, X., Zhang, P., Hao, Y., Yang, Y., Wu, X., Zhu, D., Guan, Y., 2013. Microarray gene expression profiling analysis combined with bioinformatics in multiple sclerosis. Mol. Biol. Rep. 40, 3731–3737.
Lu, P.P., Ramanan, N., 2011. Serum response factor is required for cortical axon growth but is dispensable for neurogenesis and neocortical lamination. J. Neurosci. 31, 16651–16664.
Luessi, F., Siffrin, V., Zipp, F., 2012. Neurodegeneration in multiple sclerosis: novel treatment strategies. Expert. Rev. Neurother. 12, 1061–1076 (quiz 1077).
Mao, J., Yuan, H., Xie, W., Simon, M.I., Wu, D., 1998. Specific involvement of G proteins in regulation of serum response factor-mediated gene transcription by different receptors. J. Biol. Chem. 273, 27118–27123.
McGiffert, C., Contos, J.J., Friedman, B., Chun, J., 2002. Embryonic brain expression analysis of lysophospholipid receptor genes suggests roles for s1p(1) in neurogenesis and s1p(1-3) in angiogenesis. FEBS Lett. 531, 103–108.
Meier, C., Anastasiadou, S., Knoll, B., 2011. Ephrin-A5 suppresses neurotrophin evoked neuronal motility, ERK activation and gene expression. PLoS One 6, e26089.
Miralles, F., Posern, G., Zaromytidou, A.I., Treisman, R., 2003. Actin dynamics control SRF activity by regulation of its coactivator MAL. Cell 113, 329–342.
Mizugishi, K., Yamashita, T., Olivera, A., Miller, G.F., Spiegel, S., Proia, R.L., 2005. Essential role for sphingosine kinases in neural and vascular development. Mol. Cell. Biol. 25, 11113–11121.
Moepps, B., Tulone, C., Kern, C., Minisini, R., Michels, G., Vatter, P., Wieland, T., Gierschik, P., 2008. Constitutive serum response factor activation by the viral chemokine receptor homologue pUS28 is differentially regulated by Galpha(q/11) and Galpha(16). Cell. Signal. 20, 1528–1537.
Moon, M.H., Jeong, J.K., Lee, Y.J., Park, S.Y., 2013. FTY720 protects neuronal cells from damage induced by human prion protein by inactivating the JNK pathway. Int. J. Mol. Med. 32, 1387–1393.
Moran, L.B., Graeber, M.B., 2004. The facial nerve axotomy model. Brain Res. Brain Res. Rev. 44, 154–178.
Murakami, A., Takasugi, H., Ohnuma, S., Koide, Y., Sakurai, A., Takeda, S., Hasegawa, T., Sasamori, J., Konno, T., Hayashi, K., Watanabe, Y., Mori, K., Sato, Y., Takahashi, A., Mochizuki, N., Takakura, N., 2010. Sphingosine 1-phosphate (S1P) regulates vascular contraction via S1P3 receptor: investigation based on a new S1P3 receptor antagonist. Mol. Pharmacol. 77, 704–713.
Olson, E.N., Nordheim, A., 2010. Linking actin dynamics and gene transcription to drive cellular motile functions. Nat. Rev. Mol. Cell Biol. 11, 353–365.
Osinde, M., Mullershausen, F., Dev, K.K., 2007. Phosphorylated FTY720 stimulates ERK phosphorylation in astrocytes via S1P receptors. Neuropharmacology 52, 1210–1218.
Papadopoulos, D., Rundle, J., Patel, R., Marshall, I., Stretton, J., Eaton, R., Richardson, J.C., Gonzalez, M.I., Philpott, K.L., Reynolds, R., 2010. FTY720 ameliorates MOG-induced experimental autoimmune encephalomyelitis by suppressing both cellular and humoral immune responses. J. Neurosci. Res. 88, 346–359.
Pape, M., Doxakis, E., Reiff, T., Duong, C.V., Davies, A., Geissen, M., Rohrer, H., 2008. A function for the calponin family member NP25 in neurite outgrowth. Dev. Biol. 321, 434–443.
Pelletier, D., Hafler, D.A., 2012. Fingolimod for multiple sclerosis. N. Engl. J. Med. 366, 339–347.
Perez-Cadahia, B., Drobic, B., Davie, J.R., 2011. Activation and function of immediate-early genes in the nervous system. Biochem. Cell Biol. 89, 61–73.
Perrin, F.E., Lacroix, S., Aviles-Trigueros, M., David, S., 2005. Involvement of monocyte chemoattrActant protein-1, macrophage inflammatory protein-1alpha and interleukin-1beta in Wallerian degeneration. Brain 128, 854–866.
Posern, G., Treisman, R., 2006. Actin' together: serum response factor, its cofactors and the link to signal transduction. Trends Cell Biol. 16, 588–596.
Quancard, J., Bollbuck, B., Janser, P., Angst, D., Berst, F., Buehlmayer, P., Streiff, M., Beerli, C., Brinkmann, V., Guerini, D., Smith, P.A., Seabrook, T.J., Traebert, M., Seuwen, K., Hersperger, R., Bruns, C., Bassilana, F., Bigaud, M., 2012. A potent and selective S1P(1) antagonist with efficacy in experimental autoimmune encephalomyelitis. Chem. Biol. 19, 1142–1151.
Raivich, G., Bohatschek, M., Da Costa, C., Iwata, O., Galiano, M., Hristova, M., Nateri, A.S., Makwana, M., Riera-Sans, L., Wolfer, D.P., Lipp, H.P., Aguzzi, A., Wagner, E.F., Behrens, A., 2004. The AP-1 transcription factor c-Jun is required for efficient axonal regeneration. Neuron 43, 57–67.
Ramanan, N., Shen, Y., Sarsfield, S., Lemberger, T., Schutz, G., Linden, D.J., Ginty, D.D., 2005. SRF mediates activity-induced gene expression and synaptic plasticity but not neuronal viability. Nat. Neurosci. 8, 759–767.
Reaux-Le Goazigo, A., Van Steenwinckel, J., Rostene, W., Melik Parsadaniantz, S., 2013. Current status of chemokines in the adult CNS. Prog. Neurobiol. 104, 67–92.
Riveros, C., Mellor, D., Gandhi, K.S., McKay, F.C., Cox, M.B., Berretta, R., Vaezpour, S.Y., Inostroza-Ponta, M., Broadley, S.A., Heard, R.N., Vucic, S., Stewart, G.J., Williams, D.W., Scott, R.J., Lechner-Scott, J., Booth, D.R., Moscato, P., Consortium, A.N.M.S.G., 2010. A transcription factor map as revealed by a genome-wide gene expression analysis of whole-blood mRNA transcriptome in multiple sclerosis. PLoS One 5, e14176.
Sanford, M., 2014. Fingolimod: a review of its use in relapsing–remitting multiple sclerosis. Drugs 74, 1411–1433.
Schevzov, G., Bryce, N.S., Almonte-Baldonado, R., Joya, J., Lin, J.J., Hardeman, E., Weinberger, R., Gunning, P., 2005. Specific features of neuronal size and shape are regulated by tropomyosin isoforms. Mol. Biol. Cell 16, 3425–3437.
Seijffers, R., Allchorne, A.J., Woolf, C.J., 2006. The transcription factor ATF-3 promotes neurite outgrowth. Mol. Cell. Neurosci. 32, 143–154.
Seijffers, R., Mills, C.D., Woolf, C.J., 2007. ATF3 increases the intrinsic growth state of DRG neurons to enhance peripheral nerve regeneration. J. Neurosci. 27, 7911–7920.
Slowik, A., Schmidt, T., Beyer, C., Amor, S., Clarner, T., Kipp, M., 2014. FTY720 is neuroprotective after cuprizone-induced central nervous system demyelination. Br. J. Pharmacol.
Stern, S., Haverkamp, S., Sinske, D., Tedeschi, A., Naumann, U., Di Giovanni, S., Kochanek, S., Nordheim, A., Knoll, B., 2013. The transcription factor serum response factor stimulates axon regeneration through cytoplasmic localization and cofilin interaction. J. Neurosci. 33, 18836–18848.
Stern, S., Knoll, B., 2014. CNS axon regeneration inhibitors stimulate an immediate early gene response via MAP kinase-SRF signaling. Mol. Brain 7, 86.
Stern, S., Sinske, D., Knoll, B., 2012. Serum response factor modulates neuron survival during peripheral axon injury. J. Neuroinflammation 9, 78.
Strochlic, L., Dwivedy, A., van Horck, F.P., Falk, J., Holt, C.E., 2008. A role for S1P signalling in axon guidance in the Xenopus visual system. Development 135, 333–342.
Takasugi, N., Sasaki, T., Ebinuma, I., Osawa, S., Isshiki, H., Takeo, K., Tomita, T., Iwatsubo, T., 2013. FTY720/fingolimod, a sphingosine analogue, reduces amyloid-beta production in neurons. PLoS One 8, e64050.
Tetzlaff, W., Bisby, M.A., 1990. Cytoskeletal protein synthesis and regulation of nerve regeneration in PNS and CNS neurons of the rat. Restor. Neurol. Neurosci. 1, 189–196.
Tetzlaff, W., Bisby, M.A., Kreutzberg, G.W., 1988. Changes in cytoskeletal proteins in the rat facial nucleus following axotomy. J. Neurosci. 8, 3181–3189.
Trapp, B.D., Nave, K.A., 2008. Multiple sclerosis: an immune or neurodegenerative disorder? Annu. Rev. Neurosci. 31, 247–269.
Watanabe, Y., Johnson, R.S., Butler, L.S., Binder, D.K., Spiegelman, B.M., Papaioannou, V.E., McNamara, J.O., 1996. Null mutation of *c-Fos* impairs structural and functional plasticities in the kindling model of epilepsy. J. Neurosci. 16, 3827–3836.
Wei, Y., Yemisci, M., Kim, H.H., Yung, L.M., Shin, H.K., Hwang, S.K., Guo, S., Qin, T., Alsharif, N., Brinkmann, V., Liao, J.K., Lo, E.H., Waeber, C., 2011. Fingolimod provides long-term protection in rodent models of cerebral ischemia. Ann. Neurol. 69, 119–129.
Wickramasinghe, S.R., Alvania, R.S., Ramanan, N., Wood, J.N., Mandai, K., Ginty, D.D., 2008. Serum response factor mediates NGF-dependent target innervation by embryonic DRG Sensory neurons. Neuron 58, 532–545.
Wu, X., Dong, L., Zhang, R., Ying, K., Shen, H., 2014. Transgelin overexpression in lung adenocarcinoma is associated with tumor progression. Int. J. Mol. Med. 34, 585–591.